LEVEL II

ELECTROMAGNETIC INTERFERENCE SUSCEPTIBILITY OF AIRBORNE FIBER OPTICS SYSTEMS

Georgia Institute of Technology

John P. Uyemura

APPROVED FOR PUBLIC RELEASE; DISTRIBUTION UNLIMITED

DTIC
ELECTE
JUL 2 2 1981
S   D
D

ROME AIR DEVELOPMENT CENTER
Air Force Systems Command
Griffiss Air Force Base, New York 13441

This report has been reviewed by the RADC Public Affairs Office (PA) and is releasable to the National Technical Information Service (NTIS). At NTIS it will be releasable to the general public, including foreign nations.

RADC-TR-81-62 has been reviewed and is approved for publication.

APPROVED: *Roy F. Stratton*

ROY F. STRATTON
Project Engineer

APPROVED: *David C. Luke*

DAVID C. LUKE, Colonel, USAF
Chief, Reliability & Compatibility Division

FOR THE COMMANDER: *John P. Huss*

JOHN P. HUSS
Acting Chief, Plans Office

UNCLASSIFIED

REPORT DOCUMENTATION PAGE	READ INSTRUCTIONS BEFORE COMPLETING FORM

1. REPORT NUMBER RADC-TR-81-62	2. GOVT ACCESSION NO. AD-A101 727	3. RECIPIENT'S CATALOG NUMBER

4. TITLE (and Subtitle) ELECTROMAGNETIC INTERFERENCE SUSCEPTIBILITY OF AIRBORNE FIBER OPTICS SYSTEMS	5. TYPE OF REPORT & PERIOD COVERED Phase Report, Oct 79 – Sep 80
	6. PERFORMING ORG. REPORT NUMBER N/A

7. AUTHOR(s) John P. Uyemura	8. CONTRACT OR GRANT NUMBER(s) F30602-78-C-0120

9. PERFORMING ORGANIZATION NAME AND ADDRESS School of Electrical Engineering Georgia Institute of Technology Atlanta GA 30332	10. PROGRAM ELEMENT, PROJECT, TASK AREA & WORK UNIT NUMBERS 62702F 23380 3PL

11. CONTROLLING OFFICE NAME AND ADDRESS Rome Air Development Center (RBCT) Griffiss AFB NY 13441	12. REPORT DATE May 1981
	13. NUMBER OF PAGES 98

14. MONITORING AGENCY NAME & ADDRESS(if different from Controlling Office) Same	15. SECURITY CLASS. (of this report) UNCLASSIFIED
	15a. DECLASSIFICATION/DOWNGRADING SCHEDULE N/A

16. DISTRIBUTION STATEMENT (of this Report)

Approved for public release; distribution unlimited.

17. DISTRIBUTION STATEMENT (of the abstract entered in Block 20, if different from Report)

Same

18. SUPPLEMENTARY NOTES

RADC Project Engineer: Roy F. Stratton (RBCT)

19. KEY WORDS (Continue on reverse side if necessary and identify by block number)

Fiber Optics
Electromagnetic Compatibility

20. ABSTRACT (Continue on reverse side if necessary and identify by block number)

The EMI problems associated with an airborne fiber optic communication system are examined. Interest is directed towards identifying possible noise sources and coupling channels which may exist. It is found that fiber optics transmission links can exhibit high degrees of immunity to stray EMI so long as certain precautions are taken in the original system design. Qualitative guidelines for decreasing the EMI susceptibility are given. Particular problem points are also discussed.

DD FORM 1 JAN 73 1473   EDITION OF 1 NOV 65 IS OBSOLETE

TABLE OF CONTENTS

TABLE OF CONTENTS (Continued)

ii

LIST OF ILLUSTRATIONS

LIST OF ILLUSTRATIONS

1.0 Introduction

Fiber optic transmission systems possess many features which make them more attractive than conventional hard-wire schemes. Among these characteristics are light weight, greatly increased bandwidth capabilities, and relative immunity to stray electromagnetic fields. Owing to such desirable properties, fiber optic systems are being used in many aspects of communication electronics which formerly employed standard cables for transmission lines. This conversion to an optoelectronic-based technology has been aided by the fact that existing hard-wire lines are easily replaced by fiber optic cables, and very little modification to the original system is required to provide the proper interfacing.

The objective of the study presented here was to evaluate the susceptibility of fiber optic systems to electromagnetic interference (EMI). The bulk of the work was directed towards the problem of electromagnetic interference typical in an airborne fiber optic link. However, enough generalities are included so that the results of the study can be easily extrapolated to an arbitrary environment.

Chapter 2 is concerned with establishing the basic EMI considerations required for the analysis. Section 2.1 introduces the concept of a noise system which consists of a noise source, a coupling channel, and a noise receiver; each of these is discussed in general terms. A list of standard techniques for reducing EMI levels in electronic systems is included in Section 2.2.

Chapter 3 presents the EMI analysis of optical fibers and cables. Sections 3.1 and 3.2 are condensed summaries of the wave propagation

- 1 -

analyses for step index and graded index fibers, respectively, and are included primarily for completeness. One familiar with the theory can skip these sections with no loss of continuity. In Section 3.3, the EMI susceptibility of bare fibers is examined; the same problem for fiber optic cables is analyzed in Section 3.4. Finally, Section 3.5 compares the EMI susceptibility of fiber optic cables with that for a standard coaxial transmission line.

In Chapter 4 the EMI problems particular to optoelectronic systems are examined. Section 4.1 is a discussion of the EMI susceptibility of conventional electronic circuitry, and is phrased in terms of the airborne system problem. Intrinsic noise sources are included for completeness in Section 4.1.3, and standard noise analysis is summarized in Section 4.1.4. Section 4.2 deals directly with the EMI susceptibility of solid state optoelectronics, with interest directed towards identifying noise coupling channels and their effects. In Section 4.2.1, the transmitter portion of the system is examined; it is found that this part of a fiber optic link is relatively insensitive to stray electromagnetic disturbances. Section 4.2.2 discusses the same problem as applied to fiber optic receivers. This section of the link is shown to be the most critical with respect to EMI problems in the system; methods of reducing interference levels are listed. Section 4.3 examines the possibility of EMI channels arising from the interfacing of fiber optic cables to the optoelectronic devices; this is found to give a neglible contribution to the overall EMI susceptibility of the system.

Chapter 5 is a brief summary of two relevant experiments which have been conducted for the ALOFT program. The results are discussed in terms of the analysis presented in the previous chapters.

Finally, Chapter 6 lists the conclusions reached in the study.

2.0 Fundamentals for EMI Analysis

This chapter is concerned with the basic physical considerations

needed to analyze EMI susceptibilities of both hard-wire and fiber optic

systems. The discussion will serve to introduce the terminology, in

addition to establishing a framework for the problem at hand.

2.1 The General EMI Problem

To effectively analyze an electromagnetic interference problem in

a given communication system, one must specify (a) the noise source, (b)

the coupling channel, and (c) the noise receiver. Figure 2.1 below shows

a block diagram for a general noise system. From this illustration, it

```
┌──────────────┐        ┌──────────────┐        ┌──────────────┐
│    NOISE     │   ──▶  │   COUPLING   │   ──▶  │    NOISE     │
│    SOURCE    │        │   CHANNEL    │        │   RECEIVER   │
└──────────────┘        └──────────────┘        └──────────────┘
```
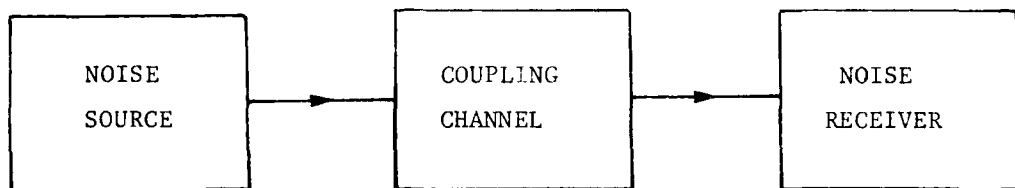
Figure 2.1

Block Diagram for the EMI Noise System [1]

is seen that there are essentially three methods available to increase the EMI immunity of the transmission system, namely, (1) locate and suppress the noise source; (2) break the coupling channel; or (3) desensitize the receiver so that the spurious noise signals are not detected. Any, or all, of these techniques may be required to insure that the EMI susceptibility is able to meet the required specifications.

2.1.1 The Noise Source

Consider first the problem of specifying the noise source. For the data transmission systems of interest here, one is concerned with the stray electromagnetic disturbances which affect the operation of a system inside an aircraft. To model the source, a "vector environmental noise field" $\vec{N}(\vec{r},t)$ is introduced to account for the unwanted signals which are not constrained by any guiding system. The vector character of $\vec{N}$ is required since the electromagnetic field is itself a vector quantity; the functional dependence on the position $\vec{r} = (x,y,z)$ and the time t accounts for the fact that the noise will be varying in both space and time. The exact form of $\vec{N}$ is determined by the problem; as an example, for a pure electromagnetic noise source, $\vec{N}$ might be taken as the Poynting vector. Since the environmental noise field $\vec{N}$ only characterizes unguided wave fields, one must also introduce a "line noise function" $L(\vec{r},t)$ which will account for EMI sources introduced on the wiring of the circuitry. The positional dependence will insure that transmission line theory is satisfied; however, for most practical problems, lumped element equivalent circuits may be used and $L \simeq L(t)$ should suffice.

Figure 2.2 on the next page illustrates in an overall sense a typical EMI source problem for a data transmission system inside an aircraft body. In the drawing, the line noise function L(t) is coupled into the transmitter and receiver modules by the power supply connections. L(t) thus accounts for generator line noise, etc., which will be introduced into the electronic signal processing networks.

The specification of the environmental noise function is a bit more complicated. It is seen that outside the aircraft body exists an external noise field $\vec{N}_{ext}$. A portion of this field will be coupled into the interior of the aircraft, either by direct penetration of the aircraft skin or through dielectric apertures in the body, such as windows. The total interior noise function $\vec{N}_{int}$ is made up of this contribution, plus any noise signals which are generated from within the aircraft itself, such as those arising from motors, etc.

When analyzing the EMI susceptibility of the data transmission system, one must locate and isolate the entrance of the environmental noise into the system. For the environmental noise introduced directly on the transmission link, it is obvious that $\vec{N}_{int}$ is the appropriate field. However, the circuitry inside the transmitting and receiving modules will be exposed to different environmental noise functions, say, $\vec{N}_{trans}$ and $\vec{N}_{rec}$, which are controlled to a certain extent by the shielding used to isolate the electronics.

It should be noted at this point that the line noise function L(t), while possessing intrinsic sources, is usually sensitive to the local environmental function since the stray EMI may be coupled onto wires and
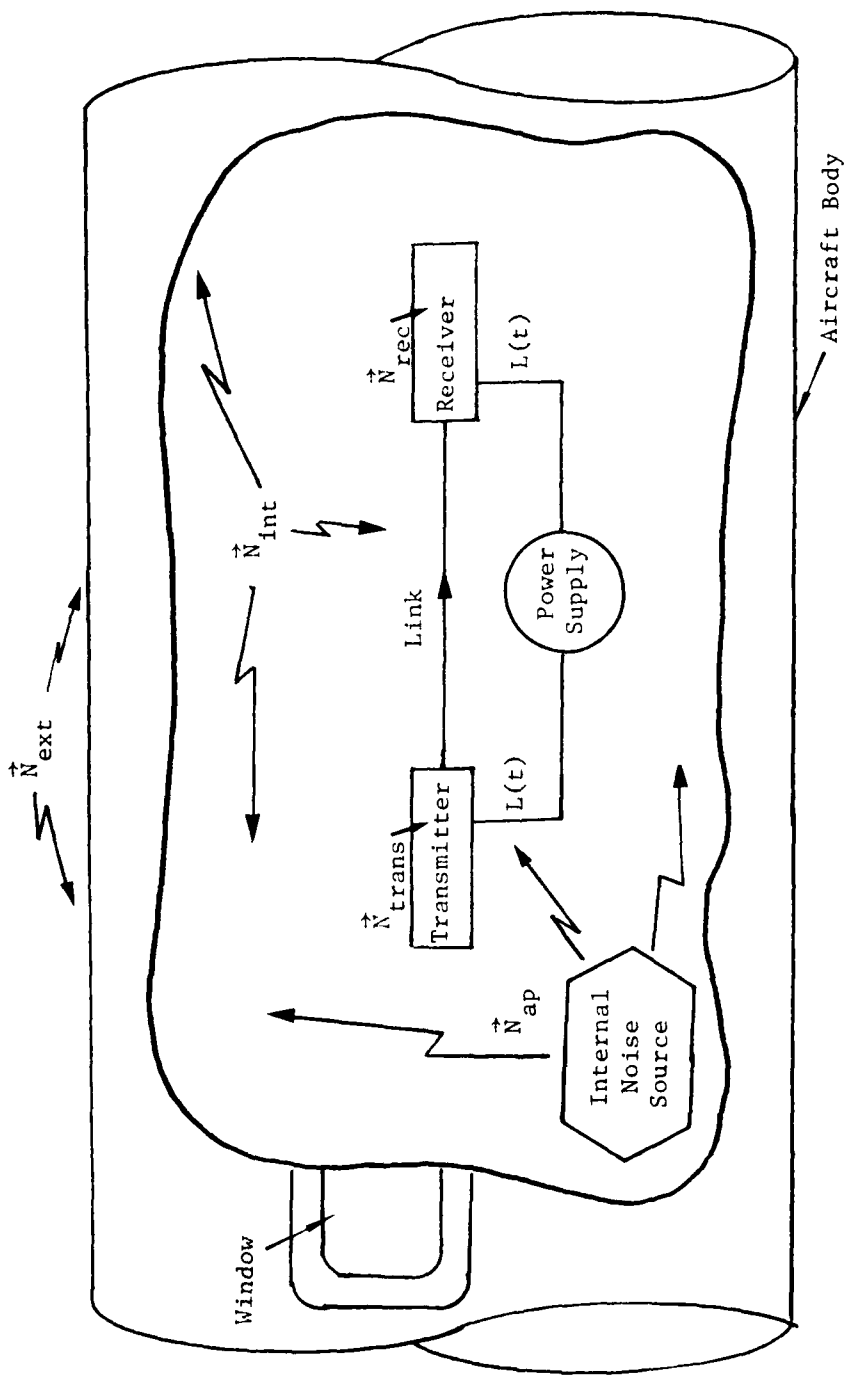
Figure 2.2

Environmental and Line Noise Sources in an Aircraft

transmitted to different parts of the system.

2.1.2 Coupling Channel Analysis

The coupling channel in the noise system of Figure 2.1 is dependent upon the position and nature of the source function. For the environmental noise described by $\vec{N}(\vec{r},t)$, one is concerned with the coupling of the fields of the EMI to the electronic circuitry and transmission link of the communication system.

The exact treatment of the coupling channel problem arising from the presence of $\vec{N}$ requires a solution to the Maxwell equations with the appropriate boundary conditions applied. Owing to the fact that practical systems rarely possess simple geometries, an exact solution is difficult, if not impossible, to obtain. For this reason, one usually approaches the problem from the viewpoint of lumped element network theory with the implied assumption that the basic conditions required for the validity of this approach are at least approximately true [2]. In terms of the environmental noise field, one may then write $\vec{N}(\vec{r},t) \simeq \vec{N}(t)$, where the point of interaction and, hence, the magnitude of the interference field, is determined by the position $\vec{r}$.

To cast the problem into equivalent network statements, the environmental coupling channel is subdivided into three subchannels according to their primary coupling processes. These are classified as electromagnetic, pure electric, and pure magnetic subchannels. The electromagnetic subchannel is one in which the entire electromagnetic field with its associated wave properties induce interference into the system. As an

- 8 -

example of an electromagnetic coupling, consider the drawing in Figure 2.3 (a) in which the leads of a transistor are exposed to stray electromagnetic disturbances. With simplicity in mind, this situation may be viewed as one in which the transistor leads act as receiving antennas, so that the EMI will induce voltages on them. This gives rise to the equivalent circuit shown in Figure 2.3 (b) in which the interference coupled into the leads of the device is represented by equivalent noise voltages.

The electromagnetic subchannel is the predominant coupling mechanism when the EMI field originates from a source which is far away from the point where the disturbance is introduced into the system. This implies that the electromagnetic subchannel deals primarily with far-zone EMI radiation fields. If, on the other hand, the EMI source and the interaction point are close to one another so that near-zone patterns must be used, it is more convenient to introduce the concept of electric and magnetic subchannels. These two classifications are relatively crude. They are not "pure" in the strictest sense owing to the fact that they are intrinsically dependent upon the electromagnetic subchannel and the line noise function $L(t)$. However, the concept of pure electric and pure magnetic subchannels are quite useful in visualizing the physical basis of certain types of interference problems, and allow one to deduce qualitative methods for the reduction of noise levels in an overall manner.

An electric subchannel exists between two points in a network when they are coupled by means of an electric field vector $\vec{E}$. A typical situation is shown in Figure 2.4 (a); the two points A and B are electri-

- 9 -
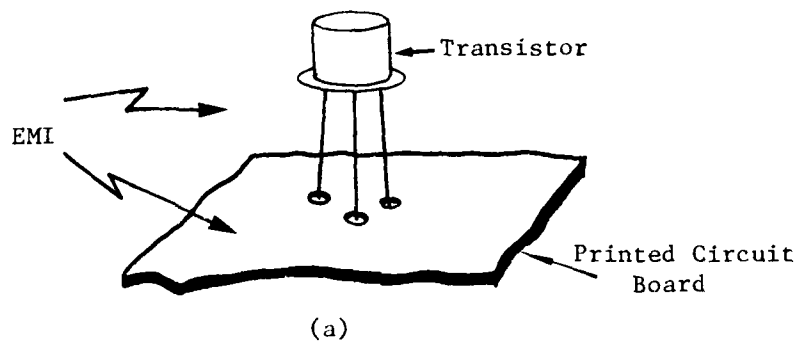
(a)

EMI Incident on the leads of a Transistor

(b)
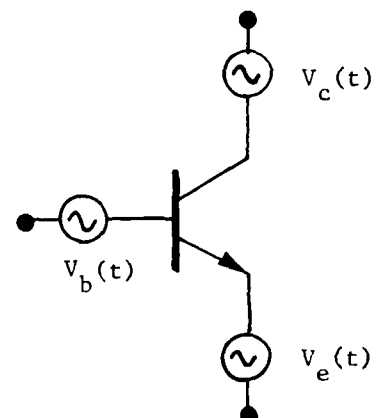
Equivalent Circuit With Noise Voltage Sources

Figure 2.3

Example of an Electromagnetic Coupling Channel
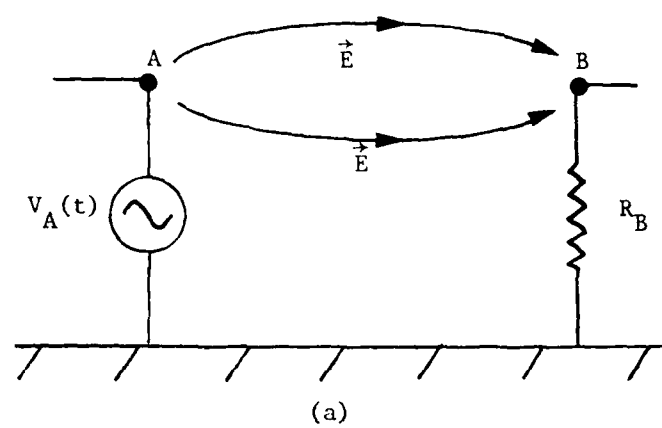
(a)

Electric Field Coupling Between Points A and B

(b)
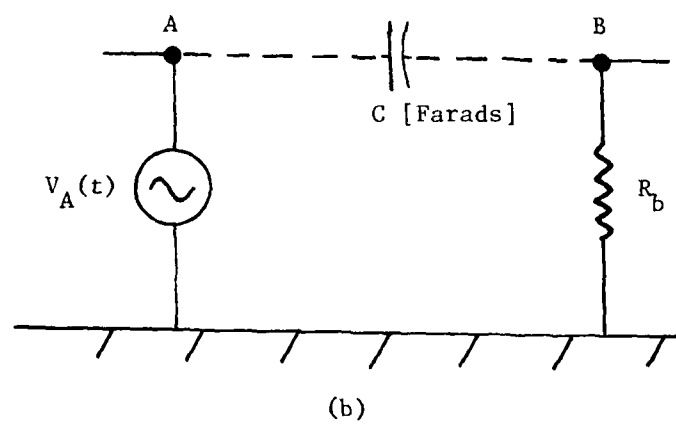
Equivalent Circuit with Capacitor C

Figure 2.4

Example of an Electric Subchannel

cally coupled to each other. This interaction may be modelled by intro-
ducing a lumped capacitance C between the points A and B, as illustrated
in Figure 2.4 (b). The physical origin of the capacitance is obvious;
however, the exact value of the element may be very difficult to compute
since it requires a solution to the Laplace equation with complicated
boundary conditions.

In the same manner, a magnetic subchannel exists between two points
that are linked by means of a magnetic flux vector $\vec{B}$. Figure 2.5 (a) on
the next page shows the case of magnetic coupling in a twin-lead cable,
where the magnetic field arising from the current in lead 1 forms a sub-
channel interaction with lead 2. In terms of an equivalent network theory,
this magnetic interaction may be represented by a mutual inductance M,
thus giving the circuit in Figure 2.5 (b). As for the case of the electric
subchannel, the exact value of the mutual inductance required for the
network equivalent is relatively difficult to compute.

A particularly important case of a magnetic subchannel is that of a
ground loop interaction. This arises from an inspection of Faraday's
Law of induction which states that

$$\oint_C \vec{E} \cdot d\vec{\ell} = -\frac{d}{dt} \int_S \vec{B} \cdot d\vec{S} \quad . \tag{2.1}$$

In this equation, C is an arbitrary closed contour described by the vector
differential line elements $d\vec{\ell}$, while S is the surface enclosed by C .
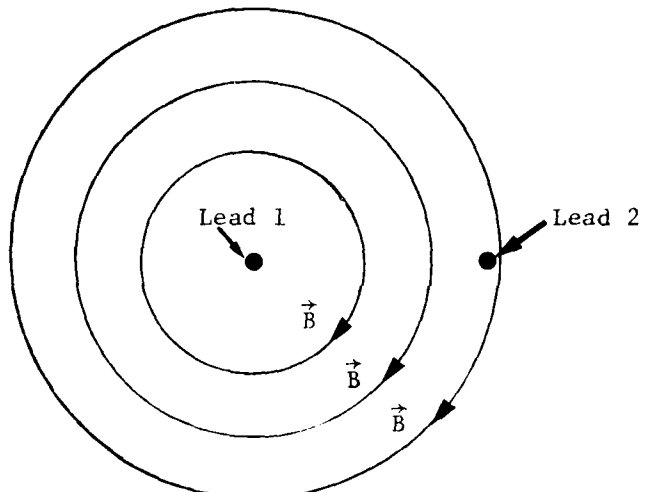
(a)

Magnetic Flux Lines From Current in Lead 1 Coupling

to Lead 2   in a Typical Twin-Lead Cable

(b)
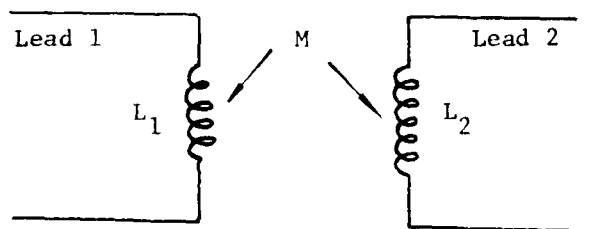
Equivalent Circuit with Mutual Inductance M Acting

as the Coupling Channel

Figure 2.5

Example of a Magnetic Subchannel Coupling

The orientation of the surface is specified by the vector differential surface area $d\vec{S}$. To see how this gives rise to a ground loop, consider the simple two resistor network shown in Figure 2.6. With the ground plane, the topology of the circuit is seen to constitute a closed contour C which bounds a surface with total area A. If a time harmonic magnetic flux vector $\vec{B}$ with an angular frequency ω pierces the surface at an angle θ to $d\vec{S}$, then equation (2.1) may be used to compute the rms value of the induced voltage as [3]

$$V_{ind} = j\omega A B_o \cos\theta \qquad (2.2)$$

where B_o is the rms amplitude of the flux. By inspection, the EMI-induced
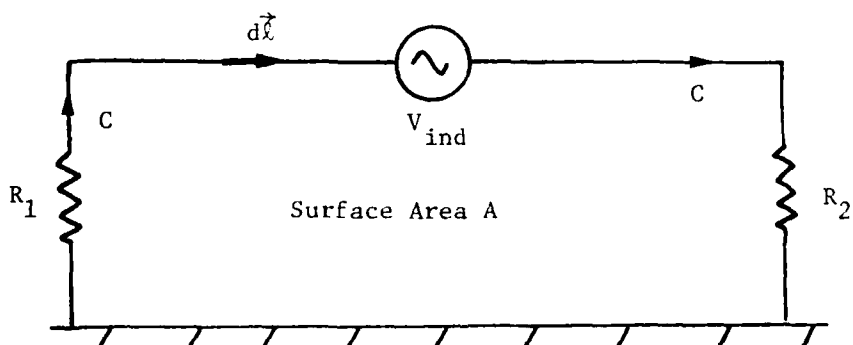
Figure 2.6

Origin of the Ground Loop Magnetic Channel

voltage depends upon the frequency, the area of the loop, the orientation of the field with respect to the loop, and the magnitude of the coupling field.

The coupling channels associated with the line noise function $L(t)$ are of a more direct nature than the environmental channels, primarily because the noise is defined as being guided along the various conduction paths in the wiring. It should be remembered, however, that a good portion of the $L(t)$ signal may be the result of environmental EMI fields which have been coupled onto the lines via the mechanisms discussed above, and subsequently transmitted to other points in the system.

The two most important channels by which $L(t)$ may be coupled into the system are (a) conductive channels, and (b) impedance couplings. An example of a conductive channel is seen in Figure 2.2 where $L(t)$ is transmitted along the power supply connections. If the system designer has no control over the power supply specifications, reasonable care must be taken to decouple or isolate $L(t)$ from the transmitter and receiver circuitry.

Impedance coupling channels are established when signals from two separate circuits or systems flow through a common impedance. A typical situation is illustrated in Figure 2.7. In the drawing, the line noise function of circuit 1, denoted by $L_1(t)$, is coupled to circuit 2 through the common ground impedance Z. Owing to the fact that both systems are grounded through the same impedance, $L_1(t)$ will induce a line noise function $L_2(t)$ in circuit 2. The amount of coupling through this channel is

- 15 -
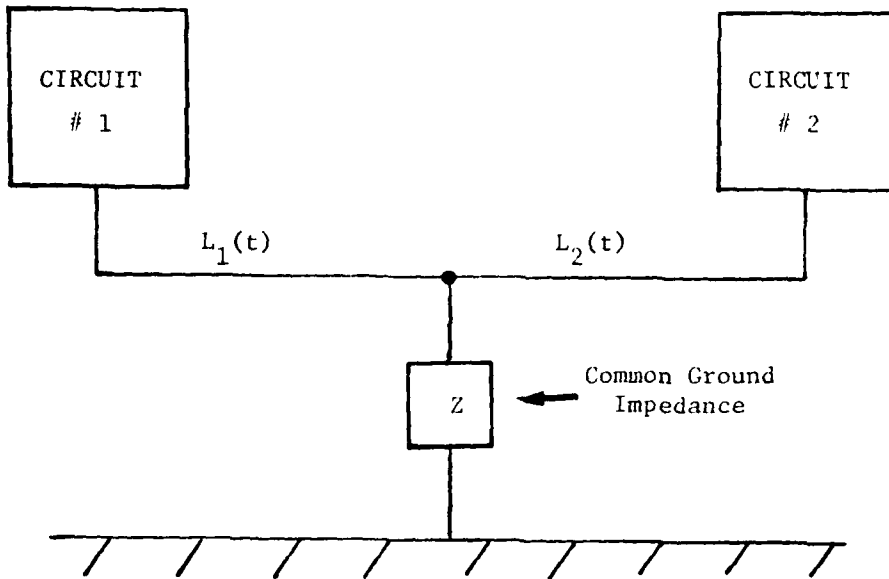
Figure 2.7

A Typical Impedance Coupling Channel

dependent upon the value of Z and the input impedances of the two circuits.

Another important impedance channel occurs when a common power supply is used for two otherwise separate systems. This is shown in Figure 2.8. Owing to the fact that no power supply is perfect in the network sense, the voltage source will have a finite impedance Z_s associated with it. The coupling channel may be established in two ways. First, if systems 1 and 2 have line noise functions $L_1(t)$ and $L_2(t)$, respectively, then the two will interact through Z_s creating a cross coupling of the noise.
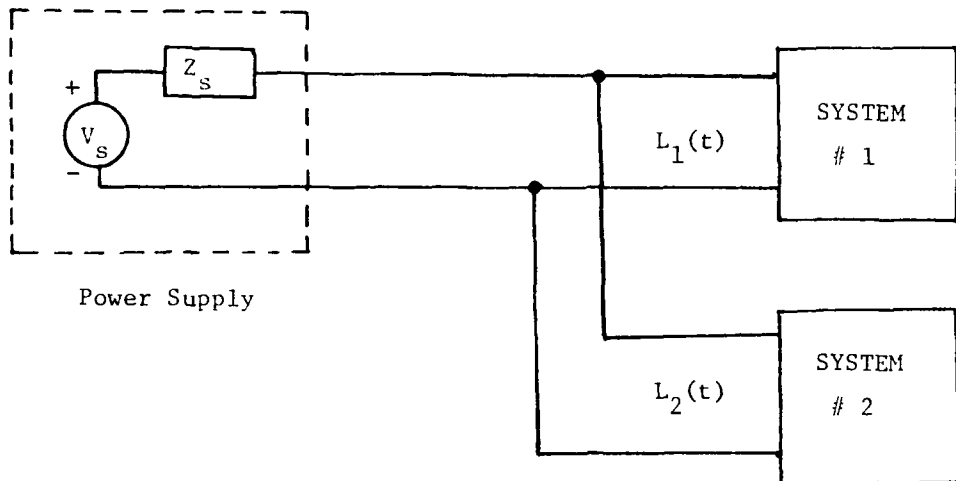
Figure 2.8

Impedance Coupling Through a Common Power Supply

Second, any variation in the amount of current drawn by one system will affect the other, since the two are coupled through the power supply. For the purposes of this report, only the cross-coupling and noise inducing mechanisms will be discussed, since power supply variations are more circuit-orientated in nature.

2.1.3 The Noise Receiver

The final block in the noise system of Figure 2.1 is the noise receiver. This can be defined in a simple manner as any point of the data transmission system which is susceptible to EMI signals arising

from either the environmental noise field or the line noise function. This definition intrinsically relates the noise receiver to the coupling channels discussed in the previous section.

2.2 Reduction of EMI Levels

In a practical transmission system, it is not possible to eliminate all unwanted EMI effects totally. Rather, the objective of efficient design is to reduce the susceptibility of the system to a point where the stray disturbances are at a tolerable level, and thus have a negligible effect on the data transmission.

The standard techniques for EMI suppression are listed below for future reference [4]:

1. Shielding
2. Grounding
3. Balancing
4. Filtering
5. Isolation
6. Separation and Orientation
7. Impedance Control
8. Cable Design
9. Cancellation

These are equally valid for both hard-wire and fiber optic systems.

3.0 EMI Susceptibility of Optical Fibers and Cables

The concept of the EMI noise system developed in the last chapter will now be applied to analyze possible EMI sources and coupling channels which may affect the transmission properties of optical fibers and fiber cable structures. As was mentioned in the Introduction, the first two sections are brief discussions of the waveguiding properties of step index and graded index fibers. The remainder of the chapter is concerned with utilizing these results to demonstrate that optical fibers intrinsically exhibit a high immunity to EMI.

3.1 Wave Propagation in Step Index Fibers

The simplest cross-sectional geometry for a practical optical fiber is the step index distribution shown in Figure 3.1. As can be seen from the drawing, this configuration is made up of a "core" region surrounded by a "cladding" of slightly lower permittivity. The higher dielectric constant of the core tends to confine most of the lightwave signal energy to this region, while the cladding serves to shield the signal from the external environment when the fiber is operated in one of its guided modes.

There are essentially two approaches which may be used to deduce the propagation characteristics of this type of lightguide, namely, the modal field analysis and the ray optics limit. Both are useful in examining the direct EMI susceptibility of the fibers, as they give a good physical understanding which allows one to qualitatively analyze any possible noise coupling channels which may exist. For this reason, the two approaches are briefly presented in the following subsections.
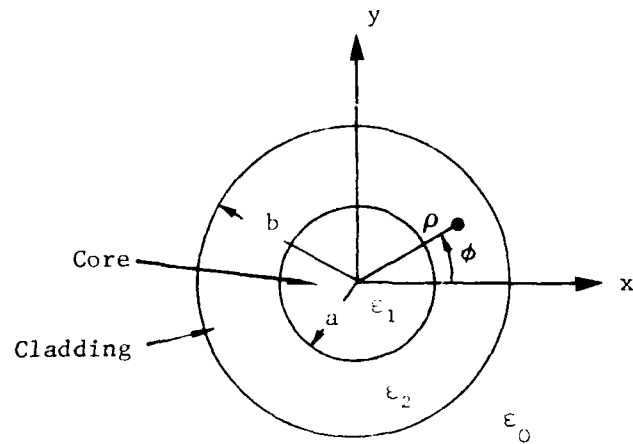
(a)

Cross-Sectional View
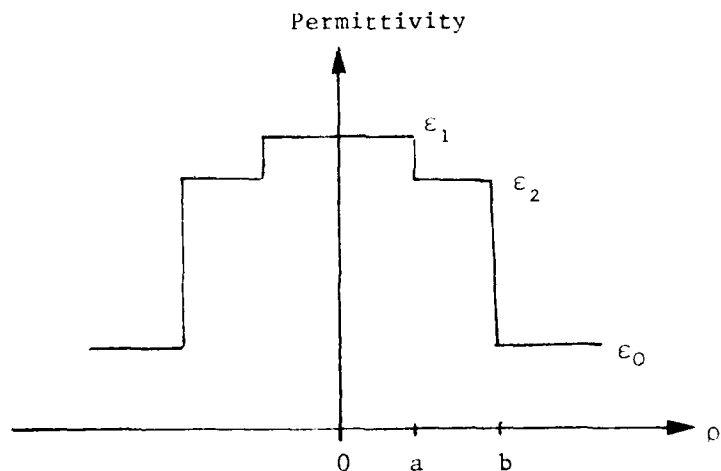
(b)

Permittivity Distribution

Figure 3.1

Geometry for a Step Index Fiber

3.1.1 Field Analysis of the Guided Wave Modes

In this approach, interest is directed towards the field properties
of the guided wave modes. The electric and magnetic fields, denoted by
$\vec{E}$ and $\vec{H}$, respectively, are found as solutions to the Maxwell differential
system such that the boundary conditions are satisfied at the interfaces.
The calculations are performed in the natural cylindrical coordinates
(ρ,ϕ,z) of the waveguide. For time harmonic field structures of frequency
ω, the wavenumber for each region is defined by $k_i^2 = \omega^2\mu\varepsilon_i$, where it is
assumed that the permeability of the entire system is given by μ. The
field computation is then reduced to finding solutions to the wave
equations

$$\nabla^2\vec{E}(\rho,\phi,z) + k_i^2 \; \vec{E}(\rho,\zeta,z) = 0$$

$$\nabla^2\vec{H}(\rho,\phi,z) + k_i^2 \; \vec{H}(\rho,\phi,z) = 0$$

$$(3.1)$$

in each region of the guide. Application of the boundary conditions to
the field vectors requires matching the tangential ϕ and z components
at the dielectric interfaces defined by $\rho = a$ and $\rho = b$; this pro-
cedure yields the eigenvalue equation for the guided mode wavenumbers
of the fiber.

In performing the calculation described above, the fields are first
written in the form [5]

$$\vec{E}(\rho,\phi,z) = \vec{E}(\rho,\phi)\ e^{-j\beta z}$$

$$(3.2)$$

$$\vec{H}(\rho,\phi,z) = \vec{H}(\rho,\phi)\ e^{-j\beta z}$$

with β the propagation constant. The field components E_z and H_z are then chosen as primary potentials for the system, with the remaining components obtained from the equations [6]

$$E_\rho = \frac{j}{k_i^2 - \beta^2}\ \left\{ \beta\ \frac{\partial E_z}{\partial \rho}\ +\ \frac{\omega\mu}{\rho}\ \frac{\partial H_z}{\partial \phi} \right\}$$

$$E_\phi = \frac{j}{k_i^2 - \beta^2}\ \left\{ \frac{\beta}{\rho}\ \frac{\partial E_z}{\partial \rho}\ -\ \omega\mu\ \frac{\partial H_z}{\partial \phi} \right\}$$

$$(3.3)$$

$$H_\rho = \frac{j}{k_i^2 - \beta^2}\ \left\{ \beta\ \frac{\partial H_z}{\partial \rho}\ -\ \frac{\omega\varepsilon_i}{\rho}\ \frac{\partial E_z}{\partial \phi} \right\}$$

$$H_\phi = \frac{j}{k_i^2 - \beta^2}\ \left\{ \frac{\beta}{\rho}\ \frac{\partial H_z}{\partial \rho}\ +\ \omega\varepsilon_i\ \frac{\partial E_z}{\partial \phi} \right\}$$

Substituting the z-components of equation (3.2) into the wave equation (3.1) allows for a separation of variables to be performed, so that the potentials assume the form

$$E_z(\rho,\phi) = E_z(\rho) \, e^{jn\phi}$$

$$\tag{3.4}$$

$$H_z(\rho,\phi) = H_z(\rho) \, e^{jn\phi}$$

with $n = 0, \pm 1, \pm 2, \ldots$ specifying the azimuthal Fourier components. The ρ-functions appearing in (3.4) are both solutions to

$$\frac{\partial^2 F(\rho)}{\partial \rho^2} + \frac{1}{\rho} \frac{\partial F(\rho)}{\partial \rho} + \left[k_1^2 - \beta^2 - \frac{n^2}{\rho^2} \right] F(\rho) = 0 \tag{3.5}$$

which is immediately recognized as the Bessel differential equation.

The guided wave modes of the step index fiber are found by writing the core potentials valid in the region $(\rho < a)$ as

$$E_z(\rho,\phi) = A_n \, J_n(u_1 \rho) \, e^{jn\phi}$$

$$\tag{3.6}$$

$$H_z(\rho,\phi) = B_n \, J_n(u_1 \rho) \, e^{jn\phi}$$

where $J_n(x)$ is a Bessel function of order n, and $u_1^2 = k_1^2 - \beta^2$ is the core radial wavenumber; A_n and B_n are arbitrary amplitudes. The cladding potentials in the region $(a < \rho < b)$ for the guided modes assume the form

$$E_{zc}(\rho,\phi) = C_n K_n(u_2\rho) e^{jn\phi}$$

$$(3.7)$$

$$H_{zc}(\rho,\phi) = D_n K_n(u_2\rho) e^{jn\phi}$$

where $u_2^2 = \beta^2 - k_2^2$, $K_n(x)$ is the modified Bessel function of the second kind, and C_n and D_n are arbitrary constants. Similarly, the exterior potentials outside the fiber $(\rho > b)$ are

$$E_{zo}(\rho,\phi) = F_n K_n(u_0\rho) e^{jn\phi}$$

$$(3.8)$$

$$H_{zo}(\rho,\phi) = G_n K_n(u_0\rho) e^{jn\phi}$$

with $u_0^2 = \beta^2 - k_0^2$ and F_n, G_n the exterior amplitudes.

The guided wave mode propagation constants, denoted by β_m, are found by using the above potentials to compute the ϕ-components of both the electric and the magnetic fields in each region. The boundary conditions of continuity are then applied at the interfaces defined by $\rho = a$ and $\rho = b$; this gives rise to a transcendental eigenvalue equation which may be solved for the allowed values of β_m. Owing to the fact that this system has been well studied in the literature (see, e.g., [7]), only the results will be presented here.

As was remarked earlier, the step index fiber is designed with a core-cladding permittivity ratio greater than one, which will tend to confine most of the electromagnetic signal field to the core region $(\rho < a)$. In terms of the radial field dependence, this is described by

standing waves in the radial (ρ) direction. As long as k_1^2 is greater than β^2, u_1 will be real (for a lossless system), so that the core potentials in (3.6) will have this property owing to the presence of the $J_n(u_1 \rho)$ functions.

If the cladding is to act as a shield for the core field distributions, the field amplitudes should decay in the region ($a < \rho < b$) for increasing values of ρ. The modified Bessel functions $K_n(u_2 \rho)$ in the cladding potentials (3.7) will insure this type of behavior so long as u_2 is real, i.e., $\beta^2 > k_2^2$. Satisfying this condition automatically implies that the fields will decay in the region ($\rho > b$) outside the fiber, since the modified Bessel functions in the exterior potentials (3.8) will have real arguments owing to the fact that $\epsilon_1 > \epsilon_2$.

With the above remarks in mind, a simplified diagram of wavenumber values can be made which shows the positions of the guided wave eigenvalues β_m. This is illustrated in Figure 3.2 for the case of four guided wave modes. The actual number of different modes which are allowed to propagate on a given step index fiber is a function of the materials, the radii, and the frequency. The plot shows that the core guided wave modes discussed above exist between k_1 and k_2, which are the intrinsic wavenumbers for the core and cladding regions, respectively. Again, these modes are characterized by radial standing wave distributions within the core ($\rho < a$), and attenuated amplitudes in the cladding and exterior regions of the fiber.

The diagram also shows the possibility of "cladding modes" in which
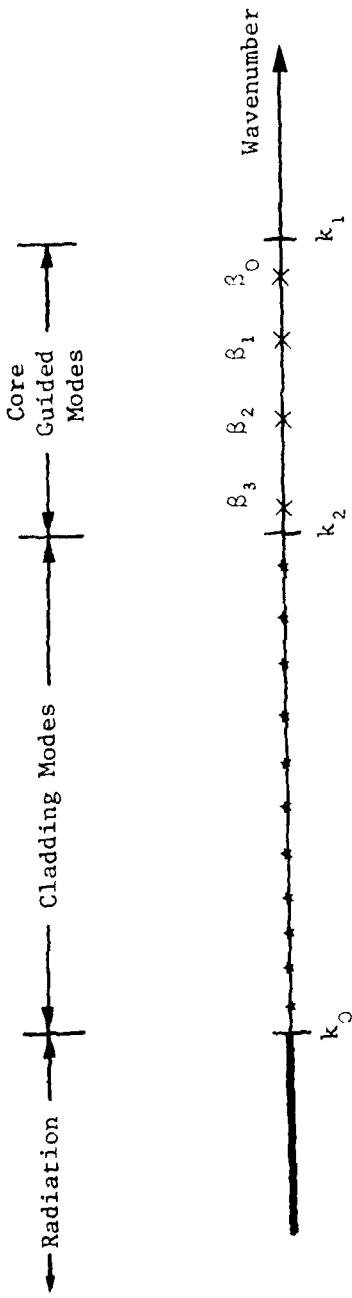
Figure 3.2

Regions of Operation for the Step Index Fiber

β falls between k_0 and k_2. For these modes, it is seen that u_1 is still real, but that u_2 will be imaginary since $k_2^2 > \beta^2$ in this region of the wavenumber line. The cladding potentials in equations (3.7) thus contain modified Bessel functions with imaginary arguments; these can be represented by linear combinations of the Hankel functions $H_n^{(1)}(x)$ and $H_n^{(2)}(x)$ [8]. The standard wave interpretation of these functions then indicates that the cladding fields will be waves propagating radially both inwards and outwards. Thus, cladding modes are characterized by radial standing waves in both the core and the cladding regions, but still decay outside the fiber. These modes may theoretically be used to transmit the lightwave signal; however, the shielding effect of the cladding is lost, so that a larger percentage of the wave field may leak to the external environment. For this reason, cladding modes are not used for long distance information transmission.

The drawing in Figure 3.2 also shows the "radiation region" for propagation constants $\beta < k_0$. In this case, u_1 in the core is real, but both u_2 and u_0 will be imaginary. The cladding fields will again establish radial standing waves as in the case of cladding modes, but now the exterior potentials in equations (3.8) will contain modified Bessel functions with imaginary arguments. So as to insure that the radiation condition is satisfied in the limit $\rho \to \infty$, the Hankel functions of the second kind $H_n^{(2)}(x)$ are used to describe the fields in the region outside the fiber, ($\rho > b$). This corresponds to an outward

propagating radial wave field which will transmit the lightwave signal energy to the external environment. Obviously, if one is interested in long distance communication with optical fibers, this type of energy loss must be avoided.

The core guided wave modes found in the above analysis are classified into four groups according to their general field characteristics. If there are no azimuthal variations in the fields, $n = 0$ and the resulting structures are termed transverse electric (TE_{om}) or transverse magnetic (TM_{om}), depending upon where $E_z = 0$ or $H_z = 0$. These are similar to the guided modes found in a metallic cylindrical waveguide used at the microwave frequencies.

If, on the other hand, $n \neq 0$, the mode structures become more complicated. The guide cannot support either a pure TE mode nor a pure TM mode for this case. Rather, both E_z and H_z are nonzero. The field configurations which fall in this category are generically termed the hybrid modes, and are designated by HE_{nm} or EH_{nm}, depending upon whether H_z or E_z is the larger component. The dominant fiber mode is the HE_{11}, which is also called the dipolar mode. It has the characteristic of zero cutoff frequency, and will be present at all times.

3.1.2 Ray Analysis of the Step Index Fiber

An alternate viewpoint for examining the guided waves in fibers is that suggested by a ray optics approach. Although it is difficult to obtain quantitative results using this type of analysis, it does have the advantage of offering a much simpler physical picture of the propa-

gation than can be found by solving the Maxwell equations.

In a step index fiber, two types of rays exist [9]: meridional rays, which pass through the guide (z) axis, and skew rays which do not have this property, but are free to move in various paths. A meridional ray is illustrated in Figure 3.3. The ray is incident on the end of the fiber at an angle θ_0 to the guide axis, and refracts at an angle θ inside the core. The ray then progresses to the core-cladding interface at an angle ϕ to the boundary normal. As long as $\phi > \theta_c$, where θ_c is the critical angle, total internal reflection will occur and the ray will be confined to the core of the waveguide. The critical angle may be computed via
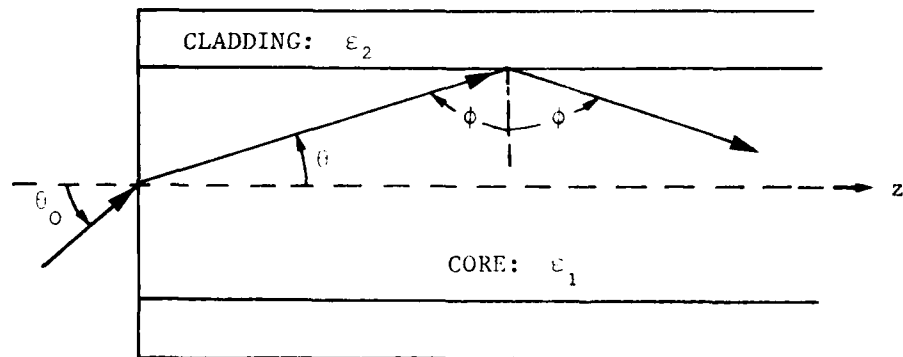
Figure 3.3

A Meridional Ray in a Step Index Fiber

$$\sin(\theta_c) = [\epsilon_1 - \epsilon_2]^{1/2} \quad . \tag{3.9}$$

Owing to the fact that this characterizes the minimum angle ϕ and hence, θ_o, required for core confinement of the ray, one defines the numerical aperture NA by

$$NA = \sin(\theta_c) \quad . \tag{3.10}$$

The NA is then a measure of "how much" light can be coupled into the end of a fiber. It is noted that if $\phi < \theta_c$, the normal processes of reflection and transmission take place at the core-cladding interface, and energy is coupled out of the core into the cladding. If total internal reflection occurs at the air-cladding interface, cladding modes will be excited. On the other hand, if the cladding ray angle is less than the air-cladding critical angle, transmission will take place at this boundary and energy will be radiated out of the fiber.

A typical skew ray is shown in Figure 3.4. As mentioned earlier, it is characterized by the fact that it never crosses the guide axis. The geometrical analysis of the ray path is slightly complicated, and will not be pursued here. The important features of skew rays are the same as for meridional rays in that the phenomenon of total internal reflection must occur at every point where the core ray touches the core-cladding interface. Otherwise, signal energy will be lost from the guide.
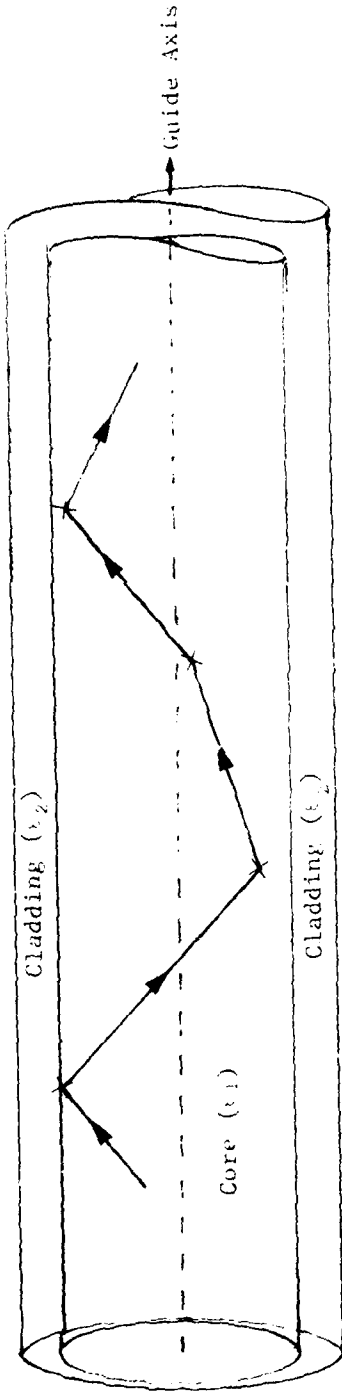
Figure 3.4

Path of a Typical Skew Ray

3.2 Graded Index Fibers

A graded index fiber is characterized by a radial core permittivity distribution $\epsilon_1(\rho)$ as illustrated by the example shown in Figure 3.3. Note that the cladding is usually a constant permittivity region; it again serves the purpose of shielding the signal field in the core from the external environment. Defining the core wavenumber

$$k(\rho) = \frac{2\pi}{\lambda} \sqrt{\epsilon_1(\rho)} \tag{3.11}$$

with λ the wavelength, the field analysis of the graded index fiber requires a solution to the core differential equation [10]

$$\frac{d^2\psi}{d\rho^2} + \frac{1}{\rho}\frac{d\psi}{d\rho} + \left\{ k^2(\rho) - \beta^2 - \frac{n^2}{\rho^2} \right\}\psi = 0 \tag{3.12}$$

where $\psi = \psi(\rho)$ is either E_z or H_z in the core   Once solutions are found, the allowed values of the propagation constant β for the guide geometry can be found.

The most straightforward approach to the problem is to use the "WKBJ" approximation [11] by writing

$$\psi(\rho) = e^{jU(\rho)} \quad . \tag{3 13}$$

Substituting this into equation (3.12) gives the equation of motion for
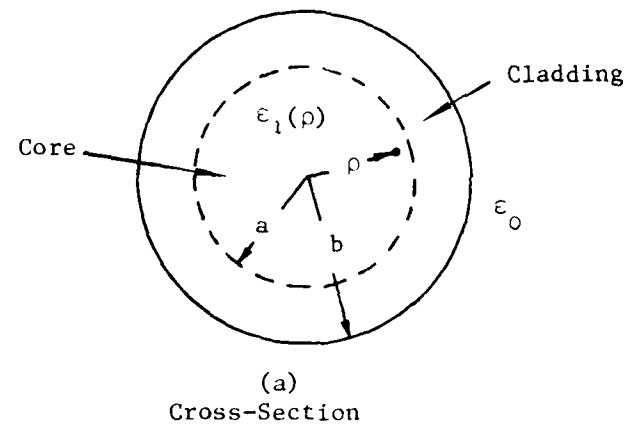
(a)
Cross-Section
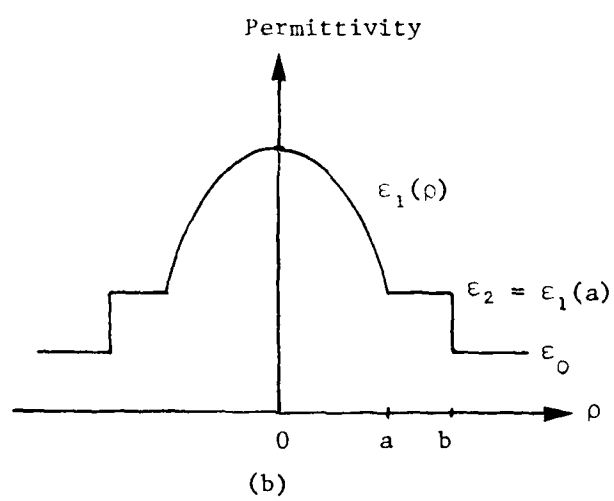
(b)

Typical Permittivity Distribution

Figure 3.5

Typical Graded Index Fiber

- 33 -

the function $U(\rho)$. Then, $U(\rho)$ is expanded in a power series in $(1/k)$ by means of

$$U(\rho) = U_0(\rho) + \frac{1}{k} U_1(\rho) + \cdots \qquad (3.14)$$

which allows for the use of successive approximations. For the description of ray motion in the graded index fiber, only $U_0(\rho)$ is needed. The field analysis, however, is much more complicated and requires a knowledge of $U_1(\rho)$.

The ray optics analysis contained in the $U_0(\rho)$ function gives rise to a plot similar to that shown in Figure 3.6; this in turn may be used to evaluate the allowed propagation numbers for the graded index fiber. In the figure, $k(\rho)$ is defined by equation (3.11), while $k(a)$ is obtained by substituting ε_2 for $\varepsilon_1(\cdot)$ in the same equation. $k(a)$ is thus interpreted as the cladding wavenumber, and is a constant for the system. Guided or bound modes exist for wavenumber values of $\beta \geq k(a)$, as shown on the diagram. The quantities ρ_1 and ρ_2 are the classical "turning points" of the system, with ray motion constrained to lie between these limits. The figure also shows the possibility of having "leaky" wave modes with propagation constants $\beta_\ell \leq k(a)$. These solutions correspond to wave modes which "leak" away from the core.

As a final point in this overview of graded index fibers, it should be pointed out that these index distributions are useful because they tend to focus the ray towards the guide axis in a continuous manner. This
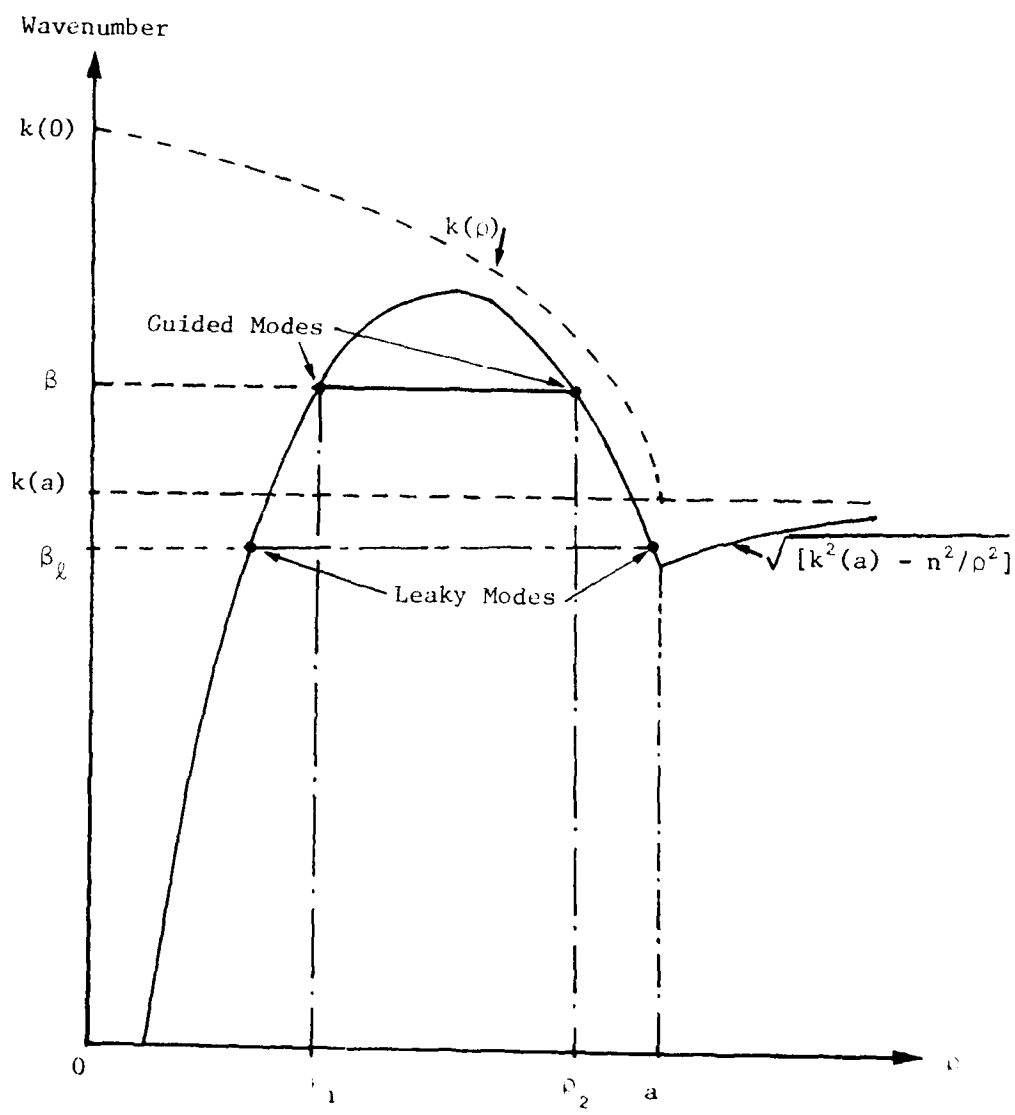
Figure 3.6

Typical Wavenumber Plot for a Graded Index Fiber

is illustrated in Figure 3.7 where the bending of the ray arises from the radial $\varepsilon_1(\rho)$ core function.
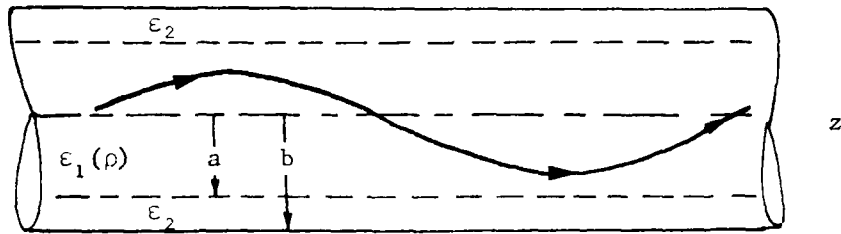
Figure 3.7

A Typical Ray in a Grade Index Fiber

3.3 EMI Susceptibility of Bare Fibers

Consider now the case where a bare optical fiber (i.e., a fiber with no extra cabling material) is employed as a communication link between the transmitter and receiver circuits. It should be noted that although such a setup is possible, bare fibers are not used in practical systems owing to the increased possibility of mechanical failure. For the purposes of this study, however, the bare fiber analysis allows for the investigation of the inherent EMI susceptibility of the fibers themselves

- 36 -

in a simple manner, and may be viewed as the "worst case" situation.

The EMI susceptibility of fibers may be discussed by invoking the Lorentz Reciprocity Theorem of electromagnetic theory [12]. When applied to the problem of wave fields in an optical fiber, this theorem says that any points in the system which allow for leakage of the signal field from the core are also points where stray electromagnetic disturbances may enter the fiber. The intrinsic EMI susceptibility of fibers may thus be ascertained by an examination of the modal field characteristics outlined in the previous two sections.

The analysis of the step index configuration in Section 3.1.1 showed that for guided (core) modes, both the cladding fields [equations (3.7)] and the exterior fields [equations (3.8)] have radial dependences described by the modified Bessel functions $K_n(x)$ with real arguments. These fields will therefore have amplitudes that decay with increasing distance ρ from the guide axis. As was pointed out earlier, this behavior is the mechanism by which the signal in the core is shielded from the environment external to the fiber.

The analysis in Section 3.1.1 shows that the larger the value of u_2, the faster the field decays in the cladding. In fact, if u_2 is sufficiently large, the exterior potential amplitudes F_n and G_n in equations (3.8) will be negligible, and there will be very little communication between the signal and the external fiber environment. Owing to the definition of u_2, this shielding will be the greatest when the modal propagation constant β_m is much larger than the cladding

wavenumber k_2. With regards to the operating regions displayed in Figure 3.2, the best core shielding occurs when β_m is close to the core wavenumber k_1.

The ray optics approach to the wave propagation in a step index fiber [Section 3.1.2] explains the shielding phenomenon in terms of critical angle arguments. If the angle ϕ of the ray is less than the core-cladding critical angle θ_c, the field will be partially transmitted into the cladding. On the other hand, when $\phi > \theta_c$, total internal reflection will keep the lightwave signal confined to the core of the guide.

Finally, the graded index fiber [Section 3.2] will protect the signal field from leaking out when the propagation constant β of the wave is greater than the cladding wavenumber $k(a)$, as illustrated in Figure 3.6. If a leaky mode is excited, some of the signal field will leak away from the core, resulting in a lower amplitude at the receiver.

The above discussion implies that the signal wave field in the core of an optical fiber can be protected from the environmental noise field $\vec{N}$ by maximizing the shielding effect of the cladding. In a practical situation, however, one has a limited amount of control over the mode selection process required in the cladding maximization procedure. This situation arises from the fact that it is difficult to specify in an a priori manner the modes which will be propagating in a fiber, owing to the "brute force" nature of the methods used to excite fiber waves in a practical system. This will be discussed in the next chapter. It is also seen that, from a theoretical standpoint, there will always be

some communication between the core and the external noise field since the cladding amplitudes never decay all the way to zero.

As was mentioned in Section 2.2, one is primarily concerned with techniques for reducing EMI levels in a system to a tolerable amount. With respect to the design of optical fibers, this can be accomplished in a straightforward manner by (1) making the cladding region relatively thick to insure sufficient decay of the field amplitudes, and, (2) choosing the core-cladding permittivity ratio to be reasonably large so as to confine the signal more efficiently. This type of philosophy is used in the design and fabrication of state-of-the-art fibers, which results in waveguides that exhibit a remarkably high degree of immunity to stray electromagnetic disturbances. For this reason, if one is careful in the selection of an optical fiber for a particular system, the EMI noise channel will be effectively cut off. There will then be very little coupling of the environmental noise field to the lightwave signal in the core.

3.4 EMI Susceptibility of Fiber Optic Cables

In the previous section it was mentioned that bare optical fibers are not used in practical systems, except perhaps for internal connections. Rather, a cable consisting of a single fiber or an array of fibers is employed for the transmission link. Typical examples of fiber optic cables are shown in Figure 3.8.

The cabling structure serves two primary purposes, namely, (1) it adds strength to the line, and (2) it provides physical protection to

(a)

Single Fiber Cable

(b)

Multifiber Cable
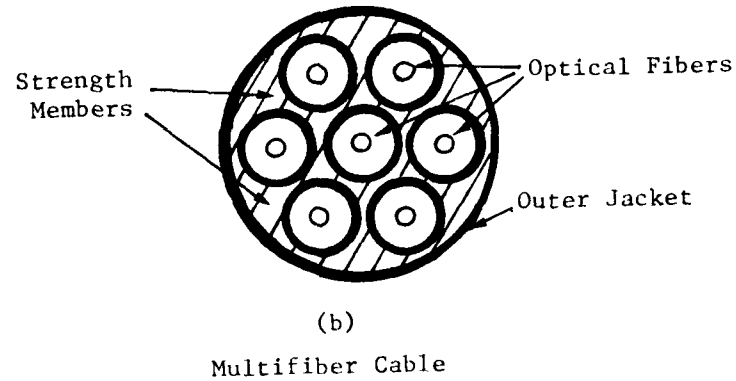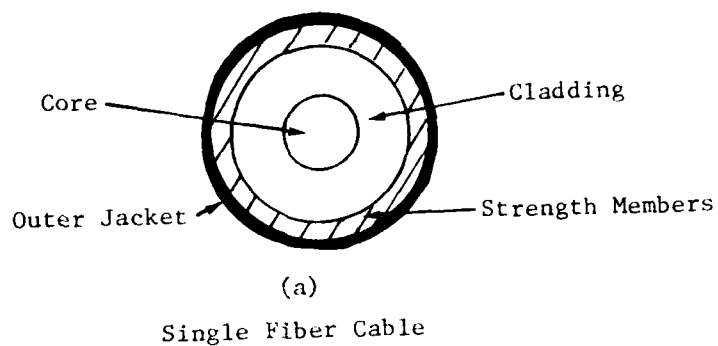
Figure 3.8

Typical Fiber Optic Cables

the surface of the fiber (or fibers) contained within the cable. The first consideration is accomplished by the addition of strength members which are less susceptible to breakage than the fiber itself. Usually, a polyethelene coating is provided, which gives additional strength. Owing to the fact that silicate glass is extremely susceptible to micro-cracks and corrosion caused by water vapor in the air, the cable strength configuration is also used to protect the fiber surfaces from exposure to the normal environment. The choice of a plastic for the outer covering enhances this protection further.

Although the cabling structures are provided for the two reasons discussed above, the extra materials serve to provide even better EMI shielding for the lightwave signal in the core. This situation arises because the material used for constructing cables also acts as an absorptive jacket which decreases the radiation outside of the trans-mission line. By the Reciprocity Theorem, one may conclude that the susceptibility to EMI is lowered, since the jacket makes the coupling channel highly resistive and lossy. Thus, the cables exhibit a high degree of immunity to the environmental noise field.

As a final note, bending losses should be considered. These arise from the fact that the analyses performed in the previous sections assumed that the fiber was an infinitely long structure which was perfectly aligned with the fiber axis. In a real-life situation, the fiber will be bent, which in turn introduces losses from the core wave signal [13]; the EMI susceptibility will thus increase. These losses,

however, are extremely small in magnitude so long as the bending radius
is large. The degree of bending must be maintained at a low level in
practical terms, since a sharp "kink" in the fiber will introduce cracks
and lead to mechanical failure. With the addition of the cabling structure,
the losses appear to be negligible with respect to EMI considerations.
However, it is well known that bending losses can introduce considerable
loss to the core wave signal over long propagation paths. At any rate,
the environmental noise field surrounding the fiber is still sufficiently
blocked by the cabling material so that the coupling is virtually nonexistant.

3.5 Fiber Optic Cables vs. Coaxial Lines

Now that the primary noise coupling channels of a fiber optic trans-
mission link have been analyzed, it is instructive to make a relative
comparison between the EMI susceptibility levels of a fiber-based system
against that encountered in a conventional hard-wire system. For the
purposes of this discussion, a coaxial cable will be chosen as a typical
hard-wire link structure. As is shown below, the use of a fiber optic
transmission line automatically eliminates a major EMI coupling channel
found in a coaxial system, namely, the ground loop.

Consider first the case where a coaxial cable is used as the
transmission link between the transmitter and receiver circuitry. This
situation is illustrated schematically in Figure 3.9. In this system
configuration, there are two possible paths which the return signal may
take when the link is in operation. One is the common ground, while the
other is the outer shield of the coaxial cable. By an appropriate choice
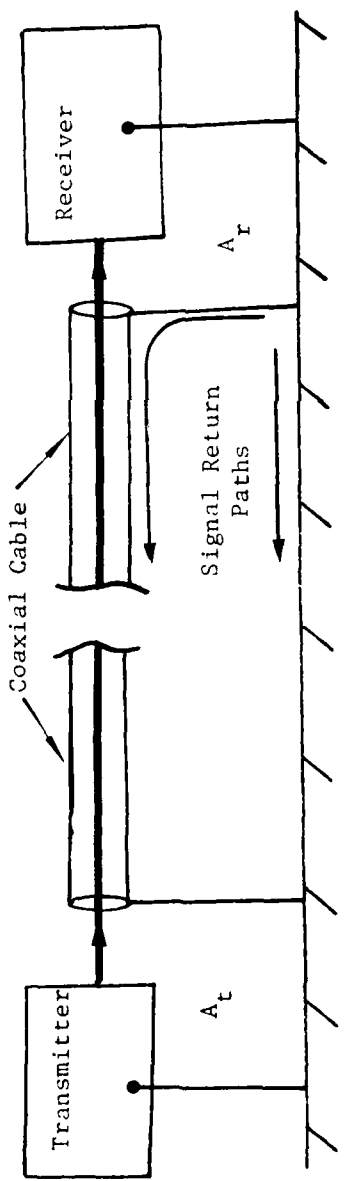
Figure 3.9

Schematic Illustration of a Coaxial

Cable System

of the operating signal properties, it is well known that the ground loop effects can be minimized, so that the coupling channel is less noticeable. However, the coupling properties of the ground loop are frequency dependent. Thus, if digital information is being transmitted, the pulses will be influenced by the environmental noise field surrounding the cable. This situation arises because a finite pulse in time may be Fourier analyzed, with the result that the frequency spectrum is essentially infinte such that the frequency domain description requires the entire spectral range. Owing to the frequency-sensitive properties of the ground loop channel, some distortion will occur in the information pulses.

Another point should be brought out concerning the system shown in Figure 3.9. It is noted that the outer conductor of the coaxial line is grounded at both the transmitter and receiver ends. For this con-figuration, it is seen that there will always exist two extra ground loops in the system simply because the cable must be connected to the transmitter and receiver circuitry. These effects can be minimized by insuring that the areas A_t and A_r are small; however, the coupling channels will never be completely eliminated. Even if a single system ground is employed, this problem will still arise.

Now suppose that instead of the coaxial cable, a fiber optic transmission link is used. Owing to the fact that the materials used to fabricate the cable are very low conductivity dielectrics, the ground loop is virtually nonexistant in the system. Thus, merely replacing the hard-wire scheme with a fiber-based link will eliminate the ground loop

interference found in a conventional system. This is a major advantage

of fiber optics, as the systems designer need not worry about this

consideration.

4.0 EMI Susceptibility of Optoelectronic Systems

The discussion in Chapter 3 served to illustrate the fact that optical fibers inherently exhibit a high degree of immunity to EMI because of their dielectric construction. In a well designed fiber optic cable, all of the EMI channels are effectively cut off, so that the transmission link itself does not contribute in any significant manner to the overall EMI susceptibility of the system.

The primary EMI coupling channels of a complete fiber optic-based transmission system are associated with the transmitter and receiver sections, and may be classified under three major headings, depending upon their origins. These are (a) the "standard" channels which occur in conventional signal processing electronics; (b) those which arise solely because of the introduction of optoelectronic devices into the networks; and (c) channels which may be open because of the interfacing of the fiber optic cables to the source or detection devices.

For the purposes of this discussion, a complete fiber optic transmission system will be represented by the block diagram shown in Figure 4.1. Note that both the transmitter and receiver sections have been split into subblocks which respectively contain the standard signal processing circuitry and the optoelectronic networks.

4.1 EMI Considerations for Conventional Electronics

The first category of EMI channels which will be examined are those which arise because of the standard signal processing circuitry. These are included for completeness of the discussion, and also because relevant
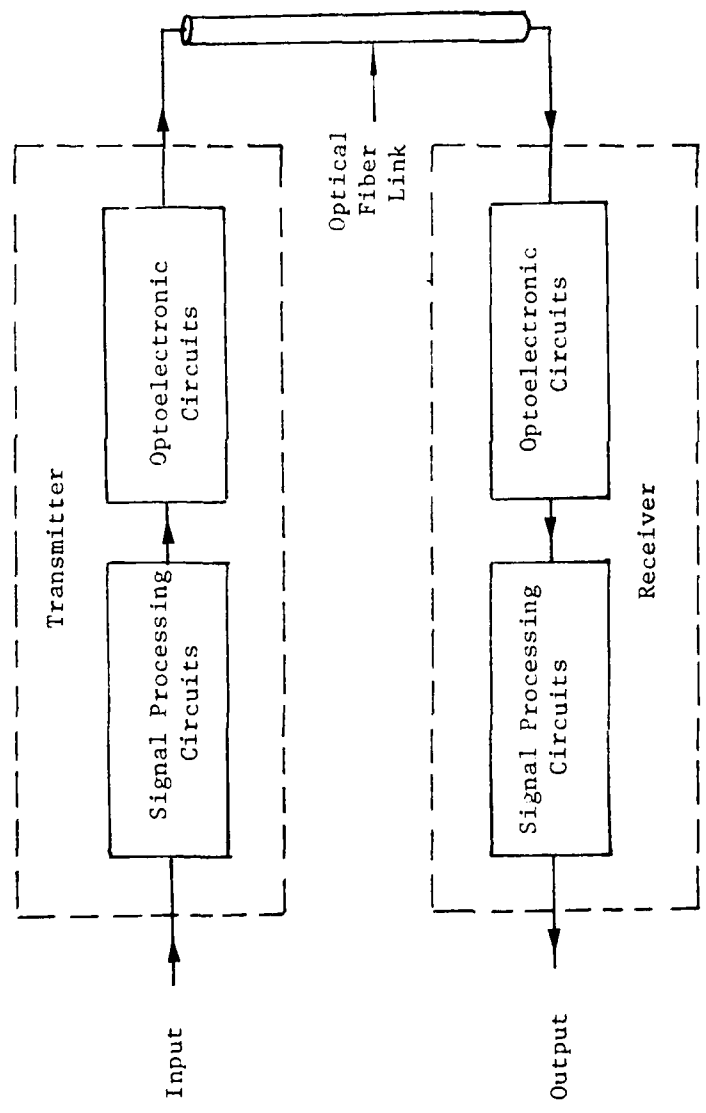
Figure 4.1

Block Diagram of a Fiber Optic System

considerations arise which are directly applicable to the optoelectronics analysis.

4.1.1 Environmental Noise Channels

The generalized environmental noise problem encountered in an airborne data transmission system was discussed in Section 2.1.1 in conjunction with the concept of noise sources. Referring to Figure 2.2 of that section, it is seen that the nature of the particular environmental EMI channels found in a given system are specified in an overall sense by the value of $\vec{N}(\vec{r},t)$ at the points where a channel may be created.

As was mentioned in Section 2.2, it is not possible to entirely eliminate noise in a practical system. With regards to environmental noise channels, there will always exist some stray electromagnetic fields because total shielding of the circuitry can never be accomplished. The circuit boards themselves will always have some exposed points which will allow for the completion of a noise coupling link.

Owing to the fact that it is not practical to make circuit boards which do not have exposed conducting points, the usual technique for increasing the EMI immunity of a system is to concentrate on reducing the magnitude of the local environmental noise field as much as possible. This will then inhibit the formation of noise channels. The reduction of the environmental noise field level is done by means of standard shielding methods in which the electronic circuitry is isolated from its noisy environment by suitable metallic enclosures. In-depth

discussions of these shielding techniques are available in the literature

(see, e.g., [14]), and will not be presented here. It is important to

note, however, that the primary source of leakage in shielded enclosures

are the seams, and also the holes that must be included for electrical

access, ventilation, etc. [14]. As will be discussed in Section 4.3,

the use of optical fibers as transmission links requires the introduction

of new apertures in the shielding that are not needed in standard

electronic systems.

The primary objective of shielding the transmitter and receiver

sections shown in Figure 4.1 is to minimize the local value of the

environmental noise field $\vec{N}$ With regards to the generalized airborne

problem in Figure 2.2, the local environmental field for both the

transmitter and receiver units can be computed from a knowledge of all

noise sources.

The interior noise field $\vec{N}_{int}$ inside the body of the aircraft can

be written as

$$\vec{N}_{int} = \alpha \vec{N}_{ext} + \vec{N}_{ap} \qquad (4.1)$$

α is the fraction of the exterior EMI field which is leaked into the

interior of the aircraft body from the outside through apertures, such

as windows, and also by discontinuities in the aircraft skin, such as

seams. The latter consideration arises because the electric fields

generated by the induced currents on the aircraft skin will be very large

- 49 -

at the points where discontinuities exist in the conducting surface. $\vec{N}_{ap}$ represents the noise field originating from sources within the aircraft itself, such as that from motors and generators. As expressed by equation (4.1), the interior noise field in a practical problem will not be controllable to any great extent, owing to the fact that structural and other considerations will usually dictate the shielding properties of the aircraft body, and also the nature of the internal noise source. One particularly interesting example is the case where the aircraft is fabricated out of composite dielectric material, as opposed to a metallic substance; for this situation, α will be quite large, so that a large percentage of the exterior noise is found inside the aircraft body.

Consider now the environmental noise field which is of importance to the circuitry. The local noise field found inside the transmitter unit can be written as

$$\vec{N}_{trans} = \beta \vec{N}_{int}$$
$$= \beta(\alpha \vec{N}_{ext} + \vec{N}_{ap}) \quad , \qquad (4.2)$$

while the local receiver field is

$$\vec{N}_{rec} = \gamma \vec{N}_{int}$$
$$= \gamma(\alpha \vec{N}_{ext} + \vec{N}_{ap}) \quad . \qquad (4.3)$$

The quantities β and γ are the transmission factors for the transmitter and the receiver, respectively, and are intrinsically less than unity.

In order to reduce the effect of the environmental noise on the circuitry of the transmission system, one would like to keep the values of β and γ as low as possible. This will then insure that the signal processing circuits are subjected to the least amount of EMI, thus reducing the effects of possible coupling channels which may exist. While the minimization of α is also desirable, it is assumed that this quantity is not controllable owing to the factors discussed above. It is noted here that if the aircraft body is designed to shield its interior from EMP (electromagnetic pulse) excitations, α will be small; this in turn aids in the EMI minimization process.

The transmission factors β and γ can never be reduced to zero for the same reasons that prohibit α from attaining this value. In particular, the transmitter and receiver shielding must have apertures to allow for information input and output. As is well known from electromagnetic theory, the field outside the shield will establish equivalent dipole distributions across the holes, which will then radiate fields into the enclosures [16]; the intensity of the radiated field will be dependent upon the geometry, and also the value of the incident field. By careful design techniques, however, it is possible to minimize the field penetration by frequency selective filtering (i.e., controlling the size and shape of the apertures) and also by keeping the number of apertures to a minimum. In addition, the locations of the holes in the

- 51 -

shielding will have an effect on the circuit susceptibility because of the vector nature of the electromagnetic noise field.

4.1.2 Line Noise Channels

The line noise function $L(\vec{r},t)$ may introduce interference into the system by either conduction or impedance channels. A typical conduction channel is that created by the interconnections among circuit boards. This is also a possible environmental noise channel, since the presence of $\vec{N}$ cannot be avoided. Again, there exist standard filtering techniques which may be used to reduce the effectiveness of conduction coupling channels [14].

With regards to an airborne system, a particularly important consideration is the channel created by the power supply connections. The wires themselves may act as conduction channels which transmit any line noise, with environmental noise being added along the way. If a single power supply is used for both the transmitter and the receiver circuitry, there is also the possibility of creating an impedance channel. With regards to the EMI viewpoint, the creation of such a channel has the potential to nullify the increased system immunity gained by using optical fibers in the first place. This situation arises because the transmitter and receiver will be connected to each other via an impedance channel which is intrinsically hard-wired. Thus, even though the fiber optic transmission link itself exhibits a high degree of EMI immunity, the system susceptibility will be greater than expected because of the power

supply coupling.

There are essentially two methods which may be used to avoid this type of transmitter-receiver interaction. The first is to insure that each system has its own power supply, with enough filtering to reduce the line noise level to a tolerable amount. If separate power supplies are not feasible, then the transmitter and receiver should be decoupled from the common supply as much as possible to inhibit the formation of an impedance channel. This could probably be done to an effective degree using standard filtering and isolation techniques.

It should also be noted at this point that the power supply connections may create ground loops through which electromagnetic subchannels could be formed. Thus, the overall problem may be more complex than the situation described here.

The line noise problem can be analyzed in much the same manner as for the environmental noise problem. Assuming that the various line noise contributions are uncorrelated, the total transmitter line noise function can be expressed as

$$ L_{trans} = \sum_n \kappa_n L_n + \sum_i \xi_i \, |\vec{N}_i| \qquad (4.4) $$

in which the coefficients κ_n give the weighting of the nth line source L_n, and ξ_i is the fraction of the ith environmental noise field $|\vec{N}_i|$ which is coupled into the transmitter via line channels. Similarly, the

receiver line noise is expressed as

$$L_{rec} = \sum_n \delta_n L_n + \sum_i \zeta_i |\vec{N}_i| \qquad (4.5)$$

with δ_n analogous to κ_n, and ζ_i analogous to ξ_i in equation (4.4). The minimization of the coefficients κ_n, δ_n, ξ_i and ζ_i is the central problem for reducing the EMI susceptibility to line noise in this terminology.

4.1.3 Intrinsic Noise Sources

In addition to the environmental noise field $\vec{N}(\vec{r},t)$ and the line noise function $L(\vec{r},t)$ introduced in Chapter 1, intrinsic noise sources should be mentioned for the discussion of the overall noise problem. Owing to their origins, these sources will contribute primarily to the line noise, but are generally viewed as sources which internally affect the operation of an electronic system and are not necessarily transmitted to other portions of the network. Owing to the fact that detailed treatments of intrinsic noise sources are available in the literature (see, e.g., [17]), only the basic properties of interest to the discussion will be presented here.

The first intrinsic noise source of interest is thermal noise, which arises from the random thermal agitation of electrons in a resistive material. Thermal noise is important as it establishes a fundamental

lower limit on the noise level present in a circuit. For a resistance
of R ohms at a temperature T (K), the open-circuit rms noise voltage
V_t produced by thermal sources is given by

$$V_t = \sqrt{4kTBR} \tag{4.6}$$

where k is the Boltzmann constant and B is the equivalent noise band-
width. In particular, for a system described by a network transfer
function A(f) with f the frequency,

$$B = \frac{1}{|A_o|^2} \int_0^\omega |A(f)|^2 \, df \tag{4.7}$$

where A_o is usually taken as being the maximum value of A(f). Thermal
noise is present in every element which contains resistance. Although
the rms noise voltage in equation (4.6) is dependent upon the system
transfer function A(f), thermal noise is characterized at the fundamental
level as having a uniform power spectral distribution, thus making it
a particular case of white noise.

Shot noise may also occur in a circuit. It is associated with
current flow across a potential barrier, and arises from the variation
of the current about an average value because of random charge carrier
emission events. For an average dc current I_{dc} through an element,

- 55 -

the rms shot noise current I_{sh} is

$$I_{sh} = \sqrt{2qI_{dc}B} \qquad (4.8)$$

where q is the electronic charge. Like thermal noise, shot noise is
a special case of white noise.

Contact noise occurs whenever two conductors are joined together,
and arises from an imperfect contact between two materials. It is known
by other names, with the more common terminologies being "flicker noise",
" 1/f noise" and "excess noise". The contact noise current I_f per
square root of bandwidth is approximated by

$$\frac{I_f}{\sqrt{B}} \simeq \frac{KI_{dc}}{\sqrt{f}} \qquad (4.9)$$

with K a constant that depends upon the materials and the geometry.
Since the contact noise power varies with frequency as 1/f, it becomes
quite significant at low frequencies.

The last type of intrinsic noise which should be introduced is
"popcorn" or "burst" noise; this source is of particular importance
in semiconductor devices. It is due to manufacturing defects in the
fabrication of semiconductor junctions, and originates from metallic
impurities which may enter the processing equipment. Popcorn noise
is characterized by discrete bursts, with burst widths varying from a

few microseconds to a few seconds; the repetition rate is random. Power densities for popcorn noise vary as f^{-n}, where n is typically 2. Since popcorn noise is current related, it is the most noticeable in high impedance circuits.

The four intrinsic noise sources described above will generally appear in the EMI problem as contributions to the line noise function L. There is also the possibility that radiation from these sources will occur, thus contributing to the environmental field $\vec{N}$; however, the magnitudes of the radiated fields will be small enough to be ignored for all practical purposes.

4.1.4 Noise Analysis for EMI

The subject of noise analysis is usually concerned for the most part with the effects of intrinsic noise sources on the information content of the signal. However, the concepts may easily be extended to give an indication of the system performance when EMI channels are formed.

The primary quantity of interest in the EMI problem is the signal-to-noise ratio (SNR) which is given by

$$SNR = \frac{P_S}{P_N} \tag{4.10}$$

with P_S the signal power and P_N the noise power, both evaluated at a common point. The noise factor F associated with a system can then be expressed as [18]

$$F = \frac{(SNR)_{input}}{(SNR)_{output}} \qquad . \qquad (4.11)$$

For an ideal noiseless system, $(SNR)_{input} = (SNR)_{output}$, and $F = 1$.
In a practical problem, however, F is always greater than unity since
the noise power can never be completely eliminated.

For a cascaded arrangement of m individual networks as shown in
Figure 4.2 on the next page, the overall noise factor is given by the
well known expression [1, 17]

$$F = F_1 + \frac{F_2 - 1}{G_1} + \frac{F_3 - 1}{G_1 G_2} + \cdots + \frac{F_m - 1}{G_1 G_2 \cdots G_{m-1}} \qquad (4.12)$$

where F_i is the noise factor for the ith stage with a gain G_i.
From this equation it is seen that if the gain G_1 of the first stage
is sufficiently large, then the overall system noise factor F is
determined primarily by the noise factor F_1 of the first stage.

This model is useful for EMI analysis when the noise voltages
induced in the system are known, or can be estimated. Assuming that
the spurious signals are uncorrelated, one can define an equivalent
total noise voltage V_N^{in} at the input of a system by

For the ith stage, F_i = noise figure, G_i = gain
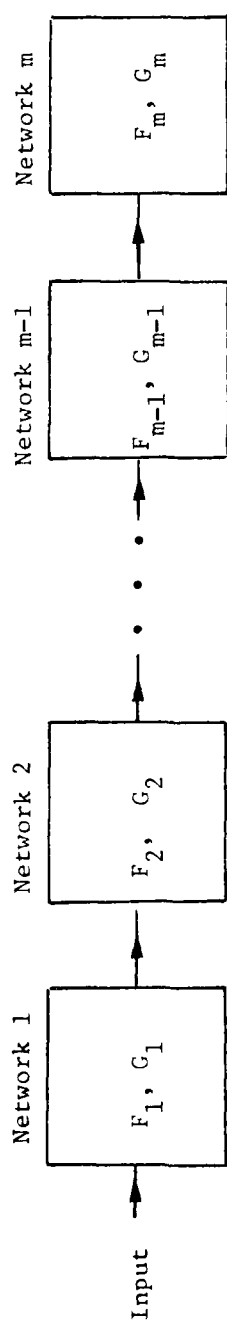
Figure 4.2

A Cascaded Arrangment of m Networks for a Typical System

$$V_N^{in} = \sqrt{\sum (V_\ell)^2} \qquad (4.13)$$

where V_ℓ is the noise voltage from the ℓth source. For noise channels which are formed in the ith stage, one can write a similar expression for the equivalent noise voltage V_N^i which contributes to F_i. It is noted in passing that if the noise voltages are correlated, one must include the cross-correlation terms in computing the total equivalent noise voltage.

4.2 EMI in Optoelectronic Circuits

This section is concerned with the EMI problems which arise when the light sources and light detectors are introduced into the electronic circuitry of a system. Since most fiber optic transmission links employ semiconductor (as opposed to vacuum or gas) devices, only these will be considered here.

4.2.1 EMI Susceptibility of the Transmitter

The transmitter assembly may be broken down into two primary ub-sections as shown in the block diagram of Figure 4.1. The introduction of a fiber optic transmission link into the system requires an opto-electronic transducer to translate the electrical signals into some form of modulated lightwave field; the portions of the circuitry which perform this task will be termed in the general sense "the" optoelectronics of

the transmitter.

The two most common light sources in use today are the light emitting diode (LED) and the semiconductor injection laser. With regards to the overall device characteristics of the two, the LED produces incoherent light with a large frequency spread, while the injection laser has a coherent wave field output with a sharp emission spectrum. In addition, the power output of an LED is limited (on the order of a few milliwatts), while a high quality semiconductor injection laser is capable of producing several watts of pulsed power at room temperature. The relative merits for using one of the other in a given system are not of particular importance to this study, and will not be considered. Rather, the analysis will be directed towards the EMI problems which come into play when these devices are incorporated into a fiber optic transmitter assembly.

4.2.1 The Light Emitting Diode

The LED is a pn junction device which is fabricated using a direct-gap semicondcutor such as GaAs or InP; the choice of materials is the major factor which determines the emission spectrum. Incoherent light is emitted from the device when the junction is forward biased, with the physical basis for this phenomenon being radiative recombination processes at the electron-hole level. Owing to the construction of the device, the current I through an LED can be computed in the ideal case from the standard Shockley equation

$$I = I_o(e^{V/V_T} - 1) \qquad\qquad (4.14)$$

where

V = applied voltage

I_o = saturation current

V_T = thermal voltage (= kT/q) .

Although the intensity of the light output is usually a complicated function of the current through the device, the biasing can be set so that the intensity is roughly proportional to the current.

A simplified LED cross-sectional arrangement, which may be taken as typical, is shown in Figure 4.3. The light rays in the drawing originate from the point X and travel towards the semiconductor-air interface. If the angle of incidence is less than the critical angle of the boundary, the light will be transmitted to the outside world and thus constitutes "usable" light for the system. In a more realistic situation, the light will also have to cross a "passification" layer of oxide which is used to protect the semiconductor surface.

For a discrete-type LED, the chip is mounted in a casing which is then mounted on a circuit board. A typical example of this is illustrated in Figure 4.4 where the diode is contained in a metallic case and a lens is provided to help focus the light. Although this particular arrangement is not generally used for a fiber optic system (since it is difficult
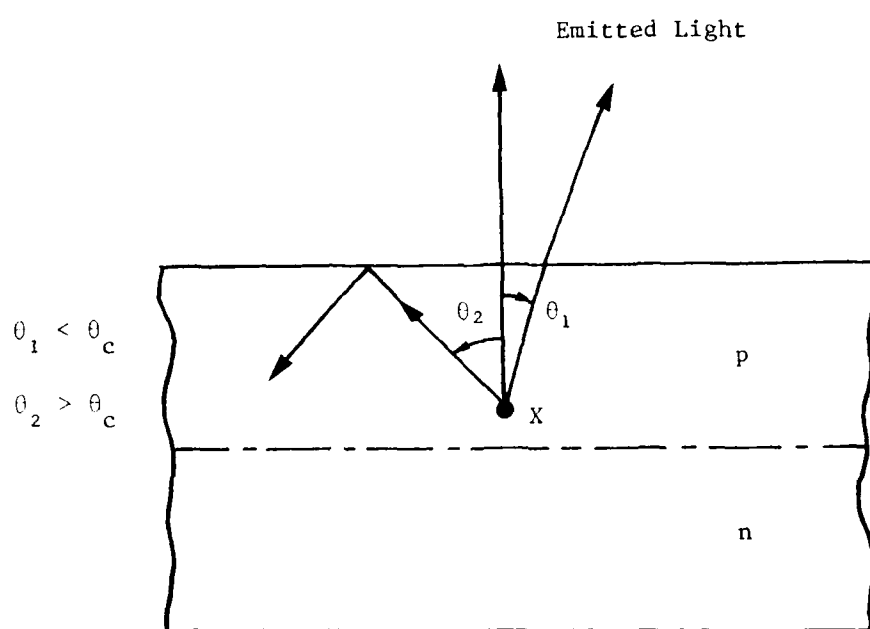
Figure 4.3

Simplified Cross-Section of an LED
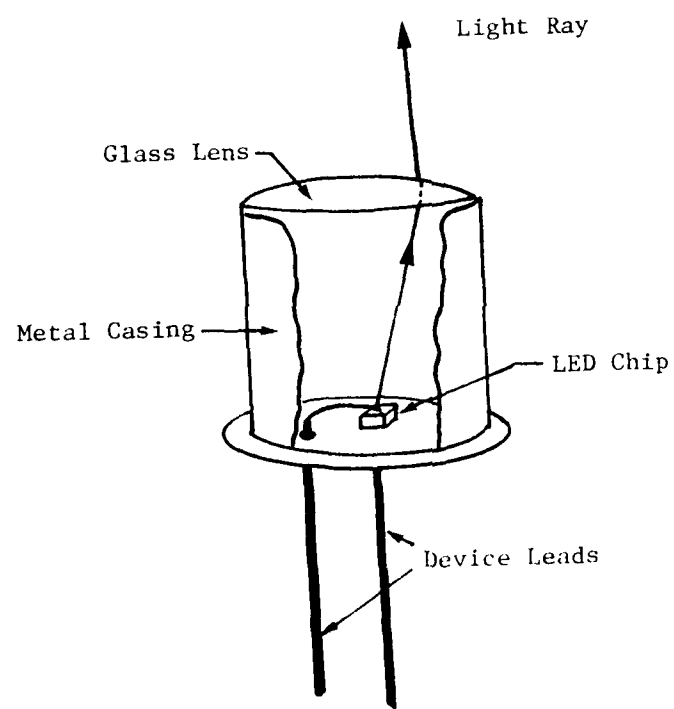
Figure 4.4

A Typical Discrete LED Geometry

to couple light into the fiber), it will suffice for the present discussion. A more practical fiber optic geometry is considered in Section 4.3.

With the brief summary above, the EMI susceptibility of systems using LED light sources can be analyzed. Consider first the physical arrangement shown in Figure 4.4. While the lens is useful in helping to focus the lightwave signals emitted from the chip, it is seen that it will also allow spurious electromagnetic interference to enter the semiconductor where electron-hole pair generation can take place; an electromagnetic (photon) noise channel will thus be established. The magnitude of the EMI induced into the system through this channel, however, will be negligible owing to the fact that the focussing properties of the lens will automatically prohibit most of the environmental noise from entering the chip area.

A more important noise channel which is created when a discrete LED is used is that associated with the mounting of the device on a circuit board. The situation will then be similar to that illustrated in Figure 2.3 (a), Section 2.1.2, for the case of a transistor. The fact that the LED has leads which are exposed to any environmental noise field which may be present inside the transmitter assembly indicates the possibility of a coupling channel. If, however, the value of β in equation (4.2) is kept small by proper shielding of the circuitry, the interference level can be reduced.

The overall problem of EMI channels arising from the mounting of

the device is most easily understood by a simple example. In Figure 4.5 a basic amplitude modulation scheme is shown. The transistor controls the diode current, and is biased into its quiescent state by resistors R_1, R_2 and R_3. Typical orders of magnitude for the diode currents are 10 - 100 milliamps, which correspond to a few milliwatts of optical power. When this system is constructed on a printed circuit board, it is seen that there will be many exposed conduction points through which environmental EMI channels can be formed. The most important interaction points
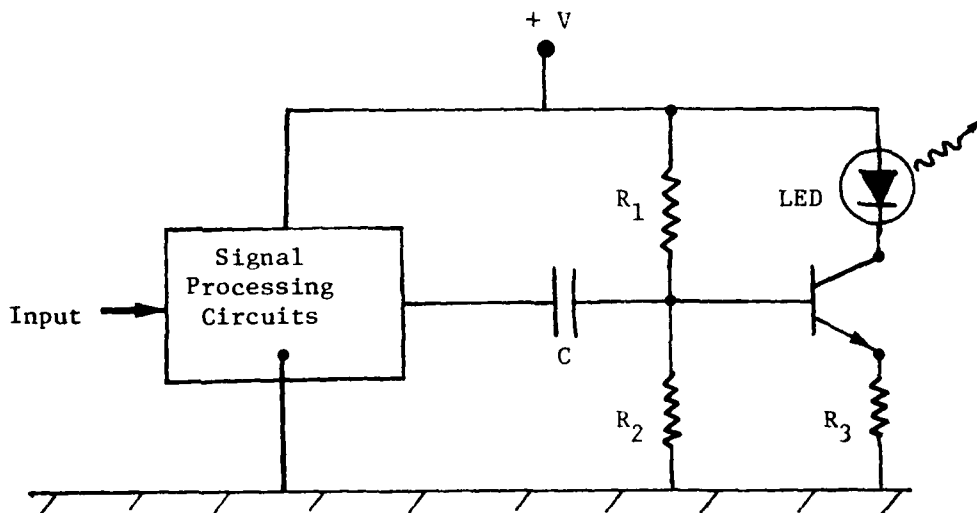
Figure 4.5

A Simple LED Amplitude Modulation Scheme

are those associated with the transistor leads, which includes the cathode

of the LED. Also note that the power supply connection and the circuit

ground can give rise to conduction and impedance channels which will

introduce line noise into the system.

Consider now the noise factor F_{mod} of the modulation stage itself.

The output SNR of this portion of the transmitter can be viewed as being

determined by the noise level in the collector current, since the intensity

of the emitted light is dependent upon the magnitude of the diode current.

The noise current in the collector is a function of (a) the magnitude of

the interference sources including the local environmental field, the

line noise and any intrinsic sources, (b) the effectiveness of the coupling

channels, and (c) the point where the coupling channels are formed. The

last consideration arises from the fact that the transistor is capable of

providing gain; thus, if noise enters the modulator through the base lead,

it will be amplified by a factor of h_{fe}, the forward current gain of

the transistor in the common emitter arrangement. This will be more

noticeable than, say, a noise signal which is directly coupled to the

emitter lead.

Although the overall EMI problem for the transmitter appears quite

complicated owing to the large number of variables involved, the system

noise factor F, which is the important quantity, can be estimated in a

very simple manner so long as care is taken in the design process. This

estimate is obtained by noting that if a small β-value is achieved cor-

responding to good shielding of the system, then the magnitude of the

environmental noise field $|\vec{N}_{trans}|$ will be small, and very little of this EMI will be coupled into the circuitry regardless of the physical construction. Similarly, if proper filtering and isolation techniques are used, then the amount of line noise entering the system can be minimized. The value of F_{mod} will then be intrinsically small. The justification for this statement can be seen by noting that the magnitudes of the EMI-induced noise voltages will be small, typically on the order of microvolts. Owing to the fact that the information signal has been amplified up to a usable level prior to reaching the modulation stage, the noise will have very little effect when compared with the magnitude of the signal variations.

Actually, the system noise factor F can be made independent of the modulation stage value by insuring that the input section of the transmitter has a high gain G_1. If this criterion is satisfied, then equation (4.12) gives that

$$F \simeq F_1 \qquad , \qquad (4.15)$$

i.e., the system noise factor is approximately equal to the noise factor of the first stage. Again, with proper care F_1 can be minimized. This leads to the conclusion that EMI levels in the transmitter should not constitute a major problem in a fiber optic system, so long as proper care is exercised in eliminating the usual noise channels which arise in standard electronic circuitry.

One final point should be mentioned in discussing the LED as a light source. For small signal variations, the Shockley equation (4.14) gives the result that the LED acts as a square-law device. One thus encounters the usual problems associated with this class of operation, namely, effects such as harmonic generation. The nonlinear properties induced by EMI coupling channels, however, should be negligible for the same reasons discussed above.

4.2.1b The Semiconductor Injection Laser

The second type of light source which is commonly used for fiber optic systems is the semiconductor injection laser. Although the physical construction of the injection laser is markedly different from that of an LED, there is very little distinction between the two geometries from the EMI viewpoint. The discussion given in the previous section is thus valid when applied to EMI coupling channels of a system which uses a laser as its light source.

There is, in fact, one operating property of the injection laser which will lead to smaller F_{mod} values than is possible with an LED. In order for the device to lase properly, the current through it must be greater than some threshold value I_{th}. Although prototype injection lasers have been built with threshold currents as low as 10 milliamps at room temperature, typical I_{th} values in state-of-the-art circuitry are on the order of 100 - 300 milliamps for CW operation. The large operating currents needed for proper laser operation thus make the noise levels even more negligible in comparison, adding an extra degree of EMI

immunity to systems which employ this type of light source.

4.2.2   EMI Susceptibility of the Receiver

The receiver assembly of a lightwave communications system can also
be divided into the two categories of standard signal processing electronics
and the optoelectronics circuitry, as shown in Figure 4.1. The opto-
electronics portion of the receiver contains a light detecting device
which translates the received optical information into electrical signals;
these are then fed into the signal processing networks.

In the previous section it was shown that the introduction of opto-
electronic circuits into the transmitter will not substantially increase
the EMI susceptibility of the system, so long as precautions are taken
with regards to shielding, etc.   This conclusion was reached because of
two main considerations. First, the transmitter system noise factor is
determined for the most part by the noise factor of the input stage
(assuming that it has a high gain); second, the noise levels induced
in the optoelectronics portions of the transmitter are much smaller than
the signal amplitudes there, so that the SNR at the light source is not
affected to any great extent.

When the EMI susceptibility of the receiver is analyzed, however,
the situation is reversed; the optoelectronic portions of the network
are found to be the primary susceptibility points of the system. This
situation arises because the light detector and its associated circuitry
necessarily form the front end (input) of the receiver. Owing to normal

insertion losses in the fiber optic link, the radiant power levels received
by the detector will be very small, perhaps as low as a few nanowatts in
a long distance system. Thus, the signal amplitudes will be small and any
noise induced into the circuit by EMI channels will increase the noise
factor of the detector stage. Since this number determines the overall
receiver noise factor, it is seen that the reduction of noise in the
receiver optoelectronic circuits is of crucial importance to the perfor-
mance of the communication link.

Interest is thus directed towards a study of the optoelectronics in
the receiver circuitry. Of the many types of solid state detectors which
are available, the PIN photodiode and the avalanche photodiode (APD) are
probably the two most commonly used devices in fiber optic systems.
Others include the solar cell, the phototransistor, and the Schottky-
barrier photodiode. The PIN photodiode is chosen here as being typical
for the purposes of the discussion.

A PIN photodiode is constructed by diffusing impurities into a
semiconductor such that there exists a strongly p-type region separated
from a strongly n-type region by a thin layer of intrinsic material. In
practice, the intermediate region is lightly doped, so that a typical
cross-section of the PIN structure appears as in Figure 4.6. A photon
which is incident on the "active area" passes through the p^+-diffusion
and into the depletion region where it creates an electron-hole pair.
Owing to the fact that electrons carry negative charge while holes have
positive charge, the built-in electric field within the depletion region

- 71 -
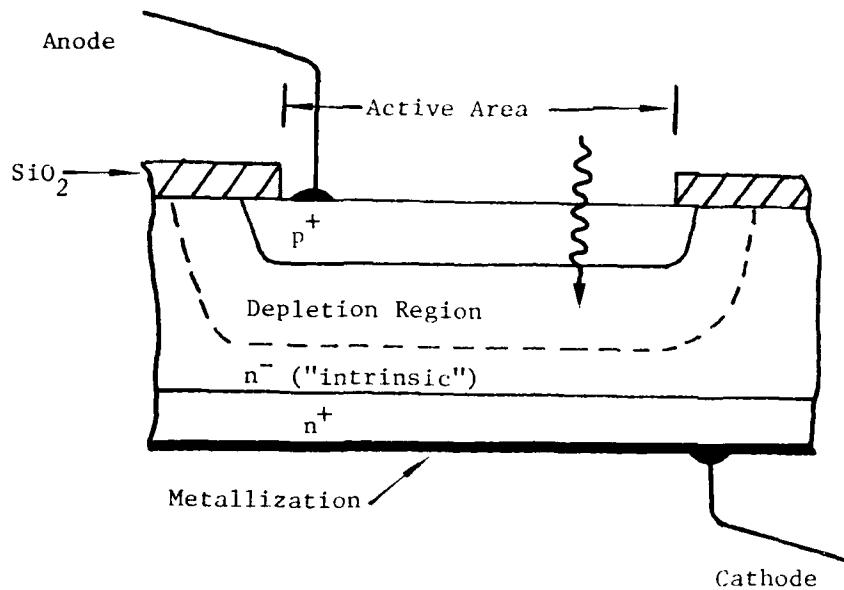
Figure 4.6

Cross-Section for a Planar Diffused PIN Photodiode

will give rise to Lorentz forces acting on the charge carriers which will

accelerate the holes towards the p^+ layer, and electrons towards the n^+

region. This establishes a photocurrent I_p through the diode. The

magnitude of I_p is proportional to the number of photons which partici-

pate in the creation of electron-hole pairs; thus, I_p is proportional

to the incident light intensity. It is noted at this point that the

energy of a photon entering the depletion region must be greater than

the value of the band gap energy E_g of the material if it is to create

an electron-hole pair. For silicon, the material which is most widely

used for detectors at the present time, E_g is approximately equal to

1.124 eV at room temperature ($T = 300^O$K). For use as a discrete device,

the PIN diode chip can be mounted in a structure identical to that shown

in Figure 4.4 for a light emitting diode. The lens now serves to focus

the incoming light onto the active area of the chip.

The PIN photodiode may be operated in one of two basic circuit

configurations; the particular mode depends upon the value of the external

bias voltage applied to the device. In the photovoltaic mode, zero bias

is applied to the diode, so that the photocurrent I_p is the output. Owing

to the high value of the zero-bias impedance, the output is ideally suited

for direct coupling into an operational amplifier (op amp). A typical

circuit arrangement is shown in Figure 4.7. In the photovoltaic mode, the
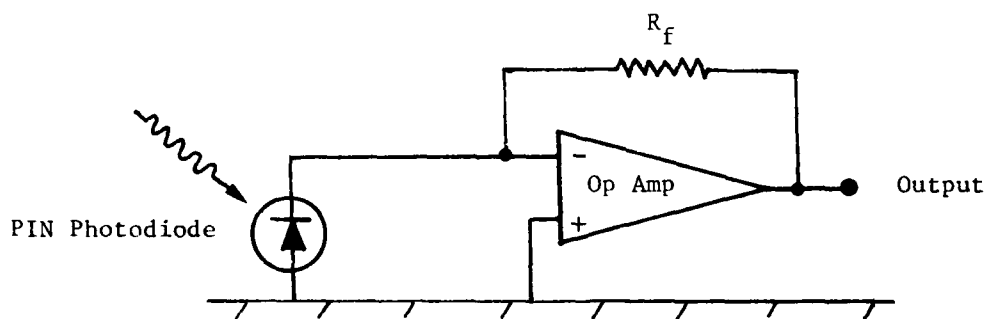
Figure 4.7

A PIN Photodiode in the Photovoltaic Mode

direct-coupling feature makes the device particularly useful for the
detection of dc light signals.

The other possible operational mode of a PIN photodiode is termed
the photoconductive mode, and occurs when the diode is reversed biased.
This mode is useful for detecting ac lightwave signals. The reverse
voltage applied to the device aids the built-in electric field, thus giving
rise to fast response times. A typical configuration is shown in Figure
4.8 below. The battery voltage V_{ex} is used to establish the proper bias
across the diode. When ac light signals are detected, the time-varying
photocurrent creates a photovoltage V_p across the resistor R. This may
then be capacitively coupled into an amplifier where the amplitude of the
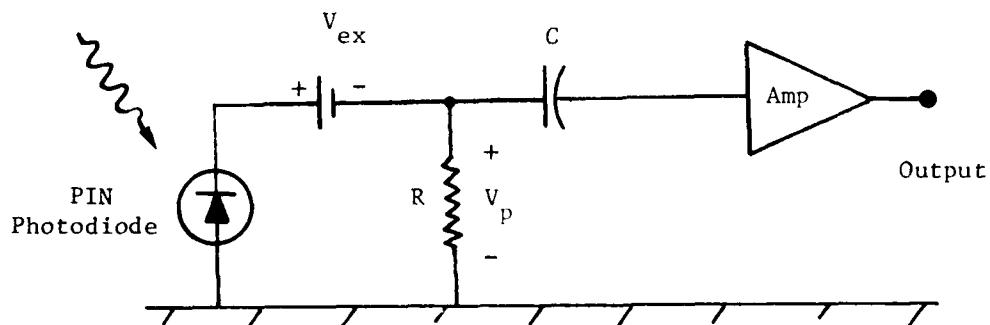
Figure 4.8

A PIN Photodiode in the Photoconductive Mode

signal is increased to usable levels. It is noted that placing the reverse bias across the junction increases the sensitivity of the device; the photoconductive mode of operation thus allows for the detection of extremely weak optical levels. Owing to this fact, the photoconductive mode is widely used in practical fiber optic systems. Another attractive feature of this operational mode is that the response of the device is almost perfectly linear.

Consider now the situation where a PIN photodiode biased into the photoconductive mode is used as the front end for a fiber optic receiver. Assuming that the diode and the amplifier in Figure 4.7 are physically discrete (i.e., that they are in separate casings), it is seen that the circuit board realization of the schematic will have many EMI susceptibility points which can adversely affect the performance of the entire communication system.

First note that the leads of the diode will be exposed to the local environmental field $|\vec{N}_{rec}|$ creating direct EMI noise channels at the input. Since the shielding factor γ in equation (4.3) can never be reduced to zero in a practical system, noise voltages will be induced into the circuitry from the leads acting as antennas with regards to the stray electromagnetic disturbances. The light levels which are detected by the photodiode are small, typically being on the order of 100 - 500 microwatts (or less). In a "good" quality PIN diode, the corresponding photocurrent I_p will be on the order of 50 - 400 microamps. Owing to these small values of signal currents, the noise currents induced by the

EMI channels in the leads may constitute a substantial fraction of the total diode current which is fed to the input of the amplifier circuitry. In addition, the casing structure will necessarily have an opening (e.g., the lens aperture in Figure 4.4) through which the lightwave signal can pass; because of this, there is an intrinsic EMI channel which can introduce noise into the diode current. If noise photon energies exceed the band gap energy E_g of the device, it will act as an efficient detector for the environmental fields which are incident on the chip.

It is also seen that the amplifier circuitry will be susceptible to the formation of EMI coupling channels, even if integrated circuits (ICs) are used. Of particular importance is any noise which is picked up by the amplifier connections and then fed into the input terminal along with the diode signal, since this will contribute towards the degradation of the SNR at the most critical point of the receiver assembly. Finally, line noise may be picked up via any conduction or impedance channels which may be formed by the normal wiring needed to complete the circuit.

In the recent literature, novel circuit designs have been presented which are directed towards minimizing the effects of intrinsic noise sources in optical receivers (see, e.g., [19]). An example of such a circuit is shown in Figure 4.9 where emphasis is on reducing thermal noise fluctuations [Section 4.1.3]. It is seen, however, that there will still exist several possible EMI coupling channels in the network, so that no great EMI advantage is gained.
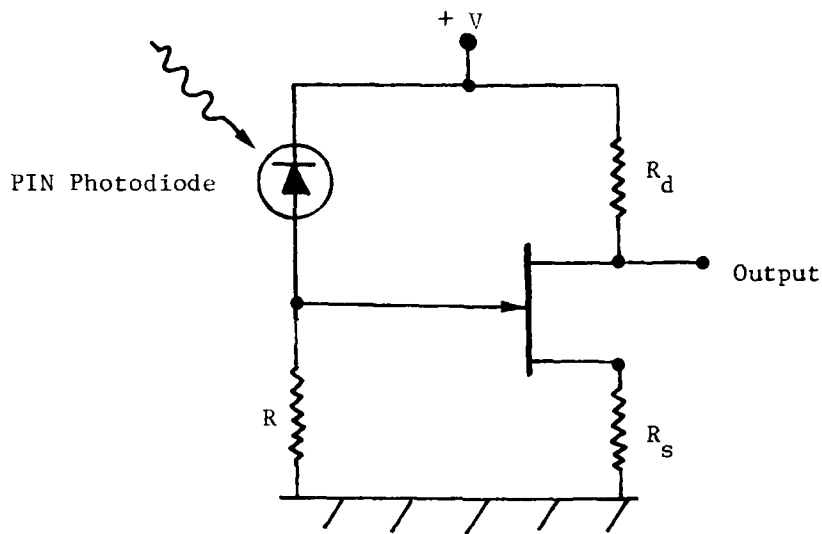
Figure 4.9

Circuit to Reduce Thermal Noise Effects

Owing to the above considerations, it is seen that a fiber optic receiver which uses a discrete detector has many susceptibility points associated with it. These are intrinsic in the system, and cannot be entirely eliminated. Since the lightwave detection circuitry constitutes the front end of the receiver, the noise factor of the system will be determined by the value in the optoelectronics section. In order to reduce the effectiveness of the EMI coupling channels, one should

(a) shield the circuitry as much as possible so as to minimize the local environmental noise field,

and

    (b)   take necessary precautions to isolate the input circuitry

         from all line noise sources.

With regards to consideration (a), it is noted that the reduction of

γ in equation (4.3) may not be sufficient to attain an acceptable SNR

at the amplifier input. It is, therefore, not unreasonable to include

an additional shield around the input circuitry to further reduce the

magnitude of the environmental noise field surrounding the detector.

In theory, proper use of the two guidelines above will allow for

"good" signal-to-noise ratios at the receiver input. If the amplifier

is designed with standard low (intrinsic) noise techniques, and also

has a large gain, then acceptable system noise factors can be obtained.

In the practical sense, however, extensive shielding and isolation is

both expensive and cumbersome. Thus, one should first quantitatively

establish a minimum system performance level, and then apply the guidelines

to the extent necessary.

As an alternate to the arrangement described above in which the

diode and the amplifier are physically discrete, consider the case where

the two are integrated into a single semiconductor chip which is then

mounted in a casing (see, e.g., [20]). For this situation, the primary

EMI channels associated with the diode leads are eliminated. The

integrated front end will therefore intrinsically exhibit a higher

degree of EMI immunity from environmental coupling channels. Thus, if

the region contiguous to the diode is excessively noisy, the detector-
amplifier integrated circuit combination should be used.

4.3 Interfacing EMI Channels

The last topic which must be examined is concerned with the possibility
of EMI coupling channels which exist because of the manner in which the
optical fiber is interfaced to the light source and detector. As was
mentioned in Section 4.2.1a, the geometry shown in Figure 4.4 for a light
emitting diode is not generally used in fiber optic systems since it is
difficult to couple light into and out of the fiber, even with the focussing
provided by the lens. Rather, a practical system will use a fiber "pigtail"
arrangement such as that shown in Figure 4.10. One end of the pigtail
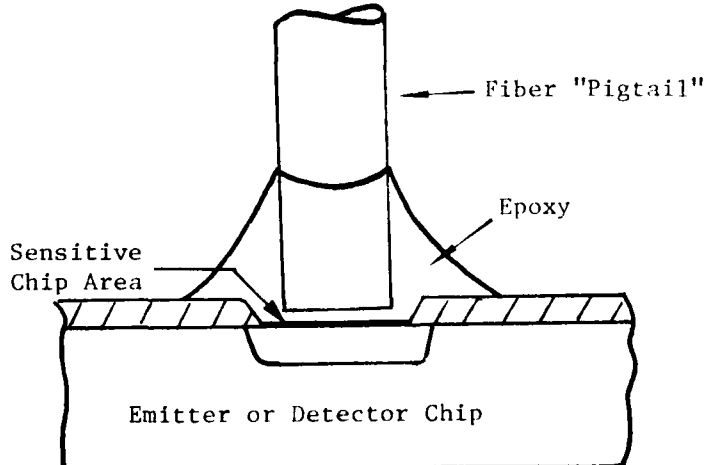
Figure 4.10

Interfacing by a Fiber Pigtail

is polished and placed in close proximity to the emitting (or detecting) area of the device; the fiber is held in place by an epoxy composition. The other end of the pigtail is used to interface the lightwave signal directly to the transmission line by means of a casing structure similar to that shown in Figure 4.11 below.
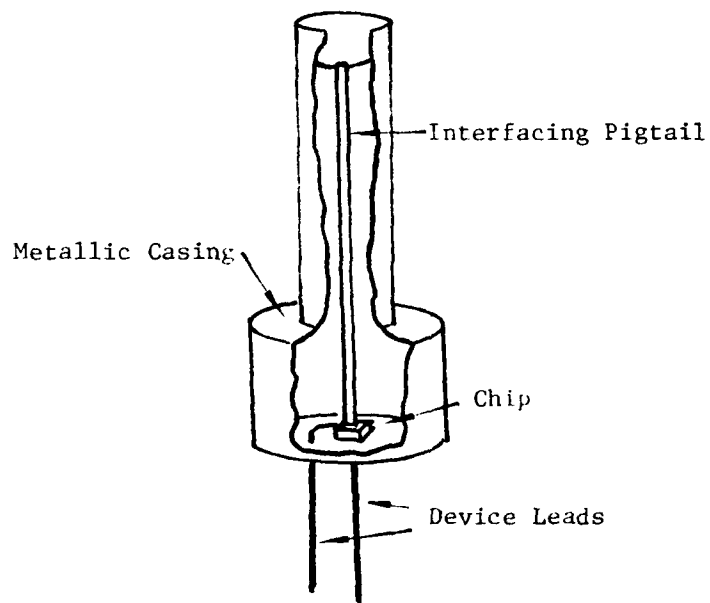

Figure 4.11

Typical Fiber Pigtail Arrangement

When compared with the lens-type scheme in Figure 4.4, the pigtail arrangement is seen to characteristically have a higher immunity to environmental EMI channels which are formed with the sensitive areas of the semiconductor chip. This is because (a) the epoxy holding the fiber pigtail in place also helps to keep the EMI from reaching the surface of the semiconductor, and, (b) the metallic casing for the entire pigtail setup acts as a shield against local system noise. Thus, if a geometrically compatible connector is used to interface the device to the fiber optic transmission cable, the environmental channels associated with the chip surface will be effectively eliminated. Note, however, that the presence of the device leads still requires the considerations discussed in the previous section.

As a final comment, it is noted that the fiber optic cable must penetrate the shielding of both the transmitter and the receiver in order to be connected to the optoelectronic circuitry. This will require extra apertures in the enclosures which would not be present in a hard-wire system. The values of β and γ in equations (4.2) and (4.3), respectively, will thus be larger than is the case for, say, a coaxial transmission line arrangement. Although this could conceivably present a problem from the EMI viewpoint, the amount of stray noise which is leaked into the interior of the shield should not be excessive, since the aperture will be at least partially blocked by the dielectric fiber. Also, if a casing such as that illustrated in Figure 4.11 is used, the container itself may be incorporated into the EMI shield, which will then eliminate this consideration entirely.

5.0 A Summary of Relevant Experiments

At the present time there is very little experimental data available which deals directly with the problems of EMI in fiber optic systems. In this section, the results of two particular experiments which have studied this problem will be examined. Since the test reports themselves are quite detailed, only a brief overview of each will be presented here.

5.1 The "A-7 Airborne Light Optical Fiber Technology (ALOFT) Demonstration Project" [21]

The main conclusion that can be extracted from this test report concerning the EMI susceptibility of fiber optic systems is that the fibers themselves do not admit to any significant EMI coupling channels. This then verifies the conclusions reached in Chapter 3.

In the ALOFT demonstration project, the direct transmission line EMI susceptibility of double-shielded cable was compared to that found for optical fibers. This was done by exposing both to a noise source, and then comparing the generated bit-error-rates in a digital link. The double-shielded cables yielded a bit-error-rate of 2.0×10^{-5} error per bit, while the fiber optic cable did not give any errors for the duration of the experimental run. The maximum bit-error-rate was thus extrapolated to about 3.9×10^{-8} errors per bit, demonstrating marked superiority over the hard-wire scheme.

5.2 The "Simulated Lightning Test and the Navy ALOFT Project" Experiment [22]

The main conclusion which can be drawn from the results of this series of tests is that a fiber optic system does exhibit a non-zero susceptibility to EMI. Furthermore, the source of the noise found in a fiber optic link originates primarily from the electronics involved.

These tests were performed at Wright-Patterson AFB, and appear to constitute the most extensive experimental investigation of the problem to date. The tests addressed three sources of EMI which arise from a simulated lightning strike on the body of an aircraft, namely, (1) EM induction into the power supply, (2) induced transients due to coupling channels on the low-level signal wiring, and (3) direct coupling into the system. Both hard-wire and fiber optic configurations were tested, with emphasis towards obtaining some quality measure with which to differentiate between the two systems.

In overview, the results indicated that sources (1) and (2) above were responsible for much of the measured transients on the fiber optic system; direct coupling as in consideration (3), however, was not measured owing to the fact that only the transmitter ends were probed. The tests indicate that the fiber optic systems experienced induced transient amplitudes which were from 550 % to 810 % lower than those measured for the hard-wire system. Another interesting result was that the frequency spectrum of the transients were different for the two arrangements; this could arise from the distinction between the optoelectronic devices and the standard electronic circuitry. Although extensive experimental data was obtained in the form of graphs, there

has not yet been any direct interpretation of the results in the quan-

titative sense owing to the complexity of the test results。

6.0 Conclusions and Recommendations

The results of this study can be summarized as follows:

(1) The fiber optic cables themselves can be made immune to EMI by

proper design. As such, they should not constitute any problems

in this area.

(2) The transmitter circuitry of a fiber optic system is susceptible

to the formation of EMI channels. However, acceptable performance

can be achieved by standard shielding and isolation techniques.

The optoelectronics involved in the transmitter assembly should

not present any major problems with regards to EMI.

(3) The light detection and amplifier portions of a fiber optic

receiver assembly are the most susceptible points for EMI coupling

in the entire fiber optic system.

If care is taken in the design process, an acceptable performance

level should be attainable.

If the environment is excessively noise, an integrated detector-

amplifier chip should be used.

(4) With a properly designed fiber optic system, there does not appear

to exist any major EMI problems which will limit performance. The

EMI properties of the fiber optic link will be greatly superior to

those found in a hard-wire system.

(5) It is recommended that a low-level effort be made to experimentally

study the EMI properties of existing fiber optic systems of interest

to the Air Force for the purpose of obtaining more quantitative

information on the problem.

In particular, interest should be directed towards (a) isolating and

classifying particular EMI coupling channels in a practical system;

(b) measurement of the relative effectiveness of each; and (c)

establishing guidelines for designing with a maximum immunity factor.

The results of such a series of tests would also be useful for a

computer simulation of the EMI problem in a fiber optic system.

7.0 References

[1]. H. W. Ott, <u>Noise Reduction Techniques in Electronic Systems</u>, Wiley-Interscience, New York, 1976.

[2]. C. A. Desoer and E. S. Kuh, <u>Basic Circuit Theory</u>, McGraw-Hill, New York, 1969.

[3]. S. Ramo, T. Van Duzer and J. R. Whinnery, <u>Fields and Waves in Communication Electronics</u>, Wiley, New York, 1965.

[4]. R. Morrison, <u>Grounding and Shielding Techniques in Instrumentation</u>, 2nd ed., Wiley-Interscience, New York, 1977.

[5]. D. Marcuse, <u>Theory of Dielectric Optical Waveguides</u>, Academic Press, New York, 1972.

[6]. N. S. Kapany and J. J. Burke, <u>Optical Waveguides</u>, Academic Press, New York, 1972.

[7]. ibid.

[8]. D. C. Stinson, <u>Intermediate Mathematics of Electromagnetics</u>, Prentice-Hall, Englewood Cliffs, N. J., 1976.

[9]. D. B. Keck, "Optical Fiber Waveguides" in <u>Fundamentals of Optical Fiber Communications</u>, M. Barnoski, Ed., Academic Press, New York, 1976.

[10]. D. Gloge, D. Marcuse and E. A. J. Marcatili, "Guiding Properties of Optical Fibers" in <u>Optical Fiber Telecommunication</u>, S. E. Miller and A. G. Chynoweth, Eds., Academic Press, New York, 1979.

[11]. A. Messiah, <u>Quantum Mechanics</u>, pp. 231-241, Wiley, New York, 1961.

[12]. J. A. Stratton, <u>Electromagnetic Theory</u>, p. 247, McGraw-Hill, New York, 1941.

[13]. D. Gloge, D. Marcuse and E. A. J. Marcatilli, "guiding Properties of Optical Fibers", Secs. 3.5, 3.12, in <u>Optical Fiber Telecommuni-</u>

cations, S. E. Miller and A. G. Chynoweth, Eds., Academic Press, New York, 1979.

[14]. R. Morrison, op. cit.

[15]. O. M. Salati, "Shielding", Chapt. 18 in Topics in Intersystem Electromagnetic Compatibility, W. W. Everett, Jr., Ed., Holt, Rinehart and Winston, New York, 1972.

[16]. R. E. Collin, Field Theory of Guided Waves, McGraw-Hill, New York, 1960; R. F. Harrington, Time-Harmonic Electromagnetic Fields, McGraw-Hill, New York, 1961.

[17]. H. L. Krauss, C. W. Bostian and F. H. Raab, Solid State Radio Engineering, Wiley, New York, 1980.

[18]. H. R. Raemer, Statistical Communication Theory and Applications, Prentice-Hall, Englewood Cliffs, N. J., 1969.

[19]. T. Witkowicz, "Design of Low-Noise Fiber-Optic Receiver Amplifiers Using J-FET's", IEEE J. Solid State Circuits, vol. SC-13, No. 1, pp. 195 – 197, 1978.

[20]. M. Ferber and J. M. Melnyk, "The Silicon Detector-Amplifier Combination", Optical Spectra, pp. 50-52, December, 1980.

[21]. R. D. Harder, R. A. Greenwell and G. M. Holma, "A-7 Airborne Light Optical Fiber Technology (ALOFT) Demonstration Project", Final Technical Report, Naval Electronics Laboratory Center, NELC/TR 2024, February 3, 1977.

[22]. Air Force Flight Dynamics Lab, Wright-Patterson AFB, "Simulated Lightining Test on the Navy Airborne Light Optical Fiber Technology (ALOFT) Demonstration Project", AD-A046 370, June 1977.

END